# Stochastic boundary conditions in the deterministic Nagel-Schreckenberg traffic model

S. Cheybani,[1,2] J. Kertész,[2,3] and M. Schreckenberg[1]
[1]*Theoretische Physik, Gerhard-Mercator Universität, D-47048 Duisburg, Germany*
[2]*Department of Theoretical Physics, Technical University of Budapest, H-1111 Budapest, Hungary*
[3]*Laboratory of Computational Engineering, Helsinki University of Technology, FIN-02150 Espoo, Finland*
(Received 10 November 1999; published 20 December 2000)

We consider open systems where cars move according to the deterministic Nagel-Schreckenberg rules [K. Nagel and M. Schreckenberg, J. Phys. I **2**, 2221 (1992)] and with maximum velocity $v_{\max}>1$, which is an extension of the asymmetric exclusion process (ASEP). It turns out that the behavior of the system is dominated by two features: (a) the competition between the left and the right boundary, (b) the development of so-called ''buffers'' due to the hindrance that an injected car feels from the front car at the beginning of the system. As a consequence, there is a first-order phase transition between the free flow and the congested phase accompanied by the collapse of the buffers, and the phase diagram essentially differs from that for $v_{\max}=1$ (ASEP).

DOI: 10.1103/PhysRevE.63.016107 PACS number(s): 05.40.−a, 45.70.Vn

## I. INTRODUCTION

Driven diffusive processes have been widely studied as prototypes of nonequilibrium systems [1–4]. They are modeled as a lattice gas and are characterized by a constant external force (e.g., electrical field), which sets up a steady current transporting information from the boundaries to the bulk of the system.

A well-known modification of the basic one-dimensional diffusive system is the asymmetric exclusion process (ASEP), which was first solved by Derrida *et al.* [5] for open boundary conditions. The ASEP is defined as follows: Consider a one-dimensional lattice of $L$ sites. Each site $i$ $(1\leqslant i \leqslant L)$ is either occupied by a particle $(\tau_i=1)$ or empty $(\tau_i=0)$. A particle on site $i$ has the probability $p$ of hopping one site to the right if site $i+1$ is empty. At the left boundary of the system a particle is injected with probability $\alpha$ if $i=1$ is empty. At the right boundary a particle on $i=L$ is removed with probability $\beta$. The ASEP can be divided into four classes according to the order in which to perform hopping, injection, and removal: (a) random-sequential update [5–8]; (b) ordered-sequential update [9,10]; (c) sublattice-parallel update [9,11–13]; (d) parallel update [14–19]. A detailed overview over all update types is given in [20].

An interesting feature of the ASEP is that phase transitions occur as a function of the model parameters. Usually there is a low-density/high-current phase and a high-density/low-current phase reminiscent of the ''free-flow'' and the ''jamming'' states in vehicular traffic [20–22]. Being a cellular automaton, the ASEP and its generalizations are well-suited to serve as simple models for traffic problems since efficient analytical and numerical techniques have been developed for their study.

As is common for traffic simulations, we will use parallel update in the following because this is the most effective among the four update types and shows the best agreement with real traffic data [23]. In Fig. 1(a) we reproduced the main results for the ASEP with parallel update: Based on investigations on global density, current, density profiles, and correlation functions, it turns out that there are two regimes, free flow and jamming, which are separated by the $\alpha=\beta$ line ($\alpha$, injection rate; $\beta$, extinction rate). All parameters have in common that they do not depend on the extinction rate $\beta$ (injection rate $\alpha$) in the free-flow (jamming) regime.

Comparing the ASEP with real traffic, however, it is obvious that phenomena such as acceleration and slowing down are not included in the model. Here, cars either do not move at all or move one site per time step. It can therefore be said that they move with maximum velocity $v_{\max}=1$. In order to get more realistic results, Nagel and Schreckenberg introduced a model [24] in which cars are able to drive with different discrete integer velocities $v$, $0\leqslant v\leqslant v_{\max}>1$.

Another interesting feature of the parallel update procedure is that it induces additional short-range correlations compared to other updating procedures. An essential part of this paper will therefore be devoted to the investigation of short-range correlation functions (Sec. V) which have already been studied in corresponding systems with periodic boundary conditions for $v_{\max}\geqslant 1$ [23–26] and in systems with open boundary conditions for $v_{\max}=1$ [15]. Moreover, it turned out that correlation functions are well suited to describe the free-flow–jamming transition [26–30].

The most significant difference between systems with open and periodic boundary conditions is the car density $\rho$. In a periodic system, the car density is a tuning parameter and the probability to find a car at a certain site $i$ is $\rho$. In systems with open boundary conditions, however, the situation is different as we have to deal with two different tuning parameters, namely the injection rate $\alpha$ and the extinction rate $\beta$, and the density is a derived parameter.

The influence of $\alpha$ and $\beta$ on the car density implies that quantities such as global density, current, and the density profile, which were studied for the ASEP ($v_{\max}=1$) in [25,31–34], show a different behavior from periodic systems. For the case $v_{\max}>1$ and open boundary conditions, however, only a few results exist. Therefore, the cases $v_{\max}=1$ and $v_{\max}>1$ in systems with open boundary conditions will be compared with each other in this paper, too.

The paper is organized as follows. In the next section the model is described. The current and the global density of the system are considered in Sec. III, in particular for the cases $\beta=1$, $\alpha=1$, and $\beta=1-\alpha$. In Sec. IV we analyze the corresponding density profiles and in Sec. V the short-range

 

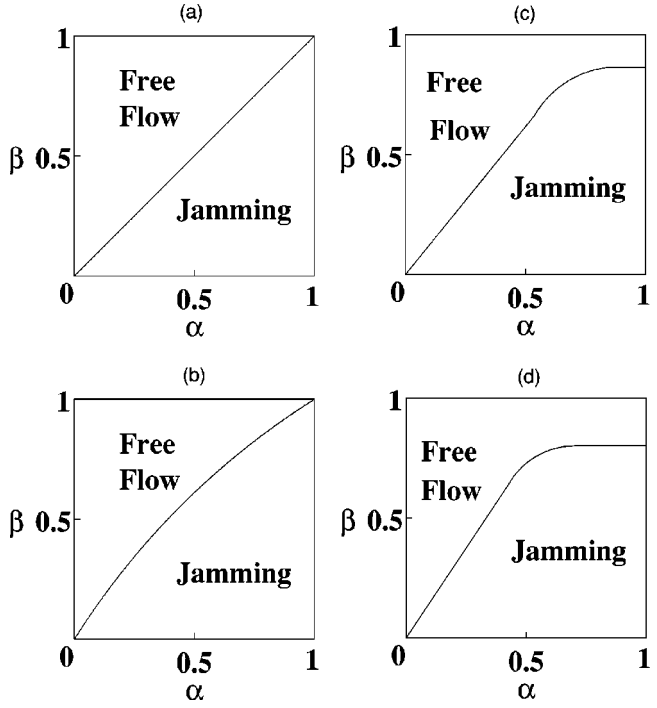


FIG. 1. (a) Phase diagram with density profiles for $v_{\max}=1$ in dependence on the injection rate $\alpha$ and the extinction rate $\beta$ (according to [14–19]). (b) Phase diagram in dependence on the injection rate $\alpha$ and the extinction rate $\beta$ ($v_{\max}=2$). (c) Phase diagram in dependence on the injection rate $\alpha$ and the extinction rate $\beta$ ($v_{\max}=3$). (d) Phase diagram in dependence on the injection rate $\alpha$ and the extinction rate $\beta$ ($v_{\max}=5$). Our investigations are focused on the cases $\beta=1$, $\alpha=1$, and $\beta=1-\alpha$ marked by dashed lines.

correlation functions. The results are summarized and discussed in Sec. VI.

## II. MODEL

Our investigations are based on a one-dimensional probabilistic cellular automaton model introduced by Nagel and Schreckenberg [24]. According to the Nagel-Schreckenberg (NS) model, the road is divided into $L$ cells of equal size and the time is also discrete. Each site can be either empty or occupied by a car with velocity $v=0,1,\ldots,v_{\max}$. All sites are simultaneously updated according to four successive steps: (i) Acceleration: increase $v$ by 1 if $v<v_{\max}$; (ii) slowing down: decrease $v$ to $v=d$ if necessary ($d$ is the number of empty cells in front of the car); (iii) randomization: decrease $v$ by 1 with randomization probability $p$ if $p>0$; (iv) movement: move car $v$ sites forward. It is obvious that the NS model is idential with the ASEP model with parallel update for maximum velocity $v_{\max}=1$. In this paper, the randomization probability is $p=0$, i.e., step (iii) (randomization) is ignored. The investigations are mainly focused on $v_{\max}=5$ but for comparison also maximum velocities $v_{\max}=2,3,4,6,7,\ldots$ are considered (see Sec. III).

Open boundary conditions are defined in the following way. The system consists of $L$ sites $i$ with $1\leqslant i\leqslant L$ (for the numerical simulations, $L=1024$). At site $i=0$, that means that out of the system a vehicle with probability $\alpha$ and with velocity $v=v_{\max}$ is created. This car immediately moves according to the NS rules. If $i=1$ is occupied by another car so that the velocity of the injected car on $i=0$ is $v=0$, then the injected car is deleted. At $i=L+1$, a ''block'' occurs with probability $1-\beta$ and causes a slowing down of the cars at the end of the system. Otherwise, with probability $\beta$, the cars simply move out of the system.

## III. CURRENT AND GLOBAL DENSITY

The phase diagrams for systems with maximum velocities $v_{\max}=2,3,5$ are shown in Figs. 1(b)–1(d). Figure 1(b) resembles the case $v_{\max}=1$ except for some deviations that are due to the fact that in systems with $v_{\max}=2$ we do not have a particle-hole symmetry as for $v_{\max}=1$. The course of the free-flow–jamming border for the case $v_{\max}=3$, on the other hand, is very different [Fig. 1(c)]. Here, the $\alpha=\beta$ line does not separate the free flow and the jamming regime. Instead, the jamming regime is larger than the free-flow regime, and for high extinction rates $\beta$ cars freely move for *all* $\alpha$. For the maximum velocity $v_{\max}=5$ these features are even more strongly developed, as is obvious from Fig. 1(d).

Let us have a closer look at the $\beta=1$ line. The current $q$ in Fig. 2(a) increases with increasing $\alpha$; for $v_{\max}\geqslant 5$, we have $q(\alpha\leqslant 0.5,\beta=1)=\alpha$. For high injection rates, however, the curves surprisingly decrease (if $v_{\max}\geqslant 4$). This phenomenon cannot be observed in systems with maximum velocities $v_{\max}=2,3$, and for $v_{\max}=4$ it is extremely weak. The maximum of the current is at $\alpha\approx 0.9$ for $v_{\max}=5$ and at $\alpha\approx 0.835$ for higher maximum velocities.

The corresponding global density $\overline{\rho}$ results from the current in Fig. 2(a) by the relation

$$\overline{\rho}(\alpha,\beta=1)=\frac{q(\alpha,\beta=1)}{v_{\max}}$$

as all cars freely move with maximum velocity $v_{\max}$.

Considering the current [Fig. 2(b)] and the global density [Fig. 2(c)] for the injection rate $\alpha=1$, we see that for $v_{\max}=2$ these quantities behave similarly to the case $v_{\max}=1$. For $v_{\max}\geqslant 3$, astonishing effects are observed which do not depend on the maximum velocity if $v_{\max}\geqslant 5$: Coming from low extinction rates $\beta$, the current for $v_{\max}\geqslant 5$ increases proportionally to $\beta$ and abruptly becomes constant at $\beta_c=0.835$. For the global density, on the other hand, the transition seems to be continuous.

Investigations of systems for large system sizes, however, show that the continuous change in the global density is just a finite-size effect: Although the curves are qualitatively the same as those in Fig. 2(c), the transition from free flow to jamming becomes more and more abrupt with increasing system size $L$. Furthermore, it turns out that the value of $\beta_c$ is slightly smaller than for $L=1024$. As a consequence, from numerical investigations of systems with large $L$ it is fair to assume that for $L\to\infty$ the current is described by

$$q(\alpha=1,\beta<\tfrac{5}{6},v_{\max}\geqslant 5)=\tfrac{4}{5}\beta \quad \text{jamming},$$

$$q(\alpha=1,\beta>\tfrac{5}{6},v_{\max}\geqslant 5)=\tfrac{2}{3} \quad \text{free flow},$$

and the corresponding global density is given by

$$\overline{\rho}(\alpha=1,\beta<\tfrac{5}{6},v_{\max}\geqslant 5)=1-\tfrac{4}{5}\beta \quad \text{jamming},$$

$$\overline{\rho}(\alpha=1,\beta>\tfrac{5}{6},v_{\max}\geqslant 5)=\frac{2}{3v_{\max}} \quad \text{free flow}.$$

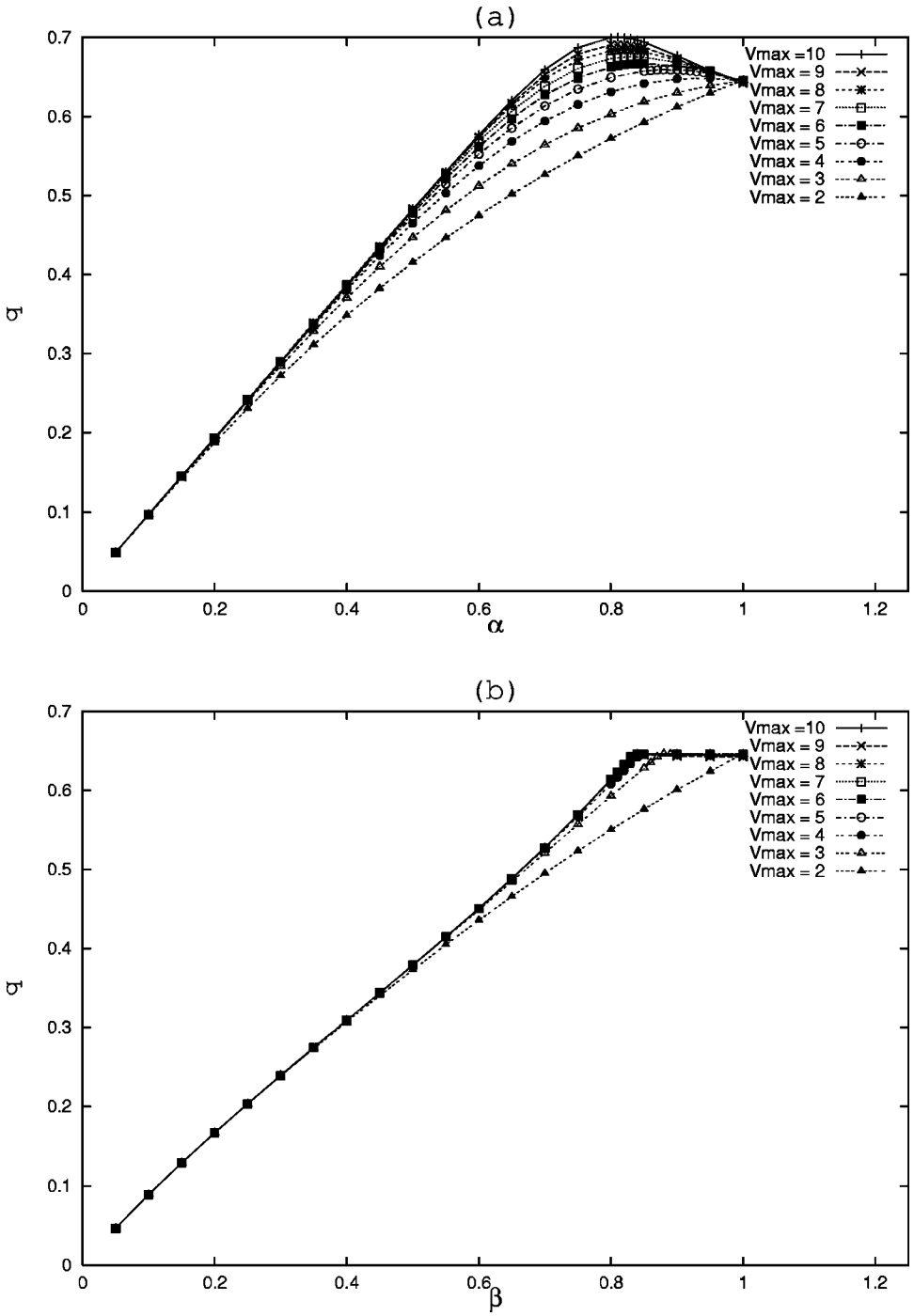


FIG. 2. (a) Current for $\beta=1$ and the maximum velocities $v_{\max}=2,3,\ldots,10$. (b) Current for $\alpha=1$ and the maximum velocities $v_{\max}=2,3,\ldots,10$. (c) Global density for $\alpha=1$ and the maximum velocities $v_{\max}=2,3,\ldots,10$.

For increasing system sizes, current and global density converge to these values which can be ''calculated'' analytically, as is demonstrated in the following. Unfortunately, there exists no extensive analytical theory of the NS model for maximum velocities $v_{\max}>1$. We must therefore restrict ourselves to a kind of bookkeeping that is nevertheless well-suited for the understanding of what is going on in the system. Furthermore, it should be emphasized that the representations of the configurations are snapshots between the slowing-down step and the movement step. This is just a convention and does not change anything in the physical meaning.

In order to get better insight into the behavior of the current and the global density, we consider the special case $\alpha=\beta=1$. The car velocity is represented by numbers in brackets, $(v)=(0),(1),\ldots,(v_{\max})$, and $k$ connected unoccupied sites by the symbol $x^k$. The first number in brackets represents the car at $i=0$ where cars are injected. Then we have the following:

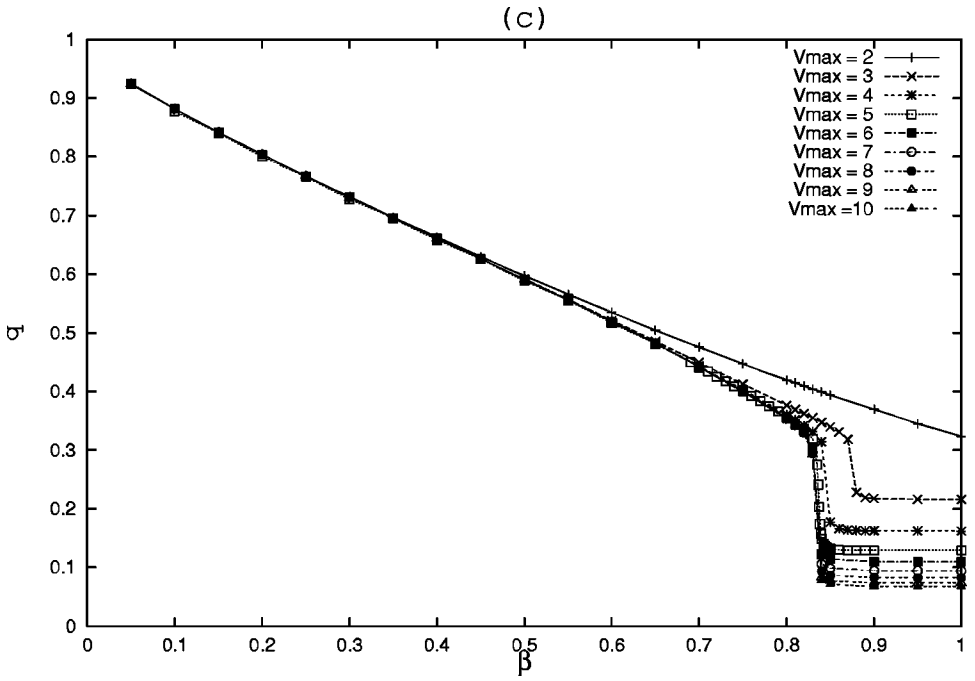


FIG. 2. (*Continued*).

$$(v_{\max})x^{L} \quad \text{for } t=0,$$
$$(v_{\max}-1)x^{v_{\max}-1}(v_{\max})x^{L-v_{\max}} \quad \text{for } t=1,$$
$$(v_{\max}-2)x^{v_{\max}-2}(v_{\max})x^{v_{\max}}(v_{\max})x^{L-2v_{\max}} \quad \text{for } t=2,$$
$$\cdots.$$

Now, a pair of consecutive cars is focused upon at the beginning of the system at time $t=n$ with $2 \geqslant n \geqslant v_{\max}-1$:

$$(v_{\max}-n)x^{v_{\max}-n}(v_{\max}-n+2)\cdots(v_{\max})x^{L-nv_{\max}} \quad \text{for } t=n.$$

The difference of the velocities of the cars is $\Delta v = v_{\text{front}} - v_{\text{back}} = 2$ and the velocity of each car increases by 1 due to the acceleration step of the NS model. Consequently, the space between the cars grows with $\Delta v t = 2t$. After $n-1$ time steps, we have

$$\cdots(v_{\max}-1)x^{v_{\max}+n-2}(v_{\max})\cdots(v_{\max})x^{L-(2n-1)v_{\max}} \quad \text{for } t=2n-1$$

and finally we find

$$\cdots(v_{\max})x^{v_{\max}+n-1}(v_{\max})\cdots(v_{\max})x^{L-2nv_{\max}} \quad \text{for } t=2n.$$

From now on, the space between the front and the back cars remains constant and consists of maximally $2(v_{\max}-1)$ empty sites due to $n \leqslant v_{\max}-1$.

The situation is different for the case $n=v_{\max}$:

$$(0)(2)\cdots(v_{\max})x^{L-v_{\max}^2} \quad \text{for } t=v_{\max}.$$

According to the left boundary conditions, the car at site $i=0$ with velocity $v=0$ is deleted and a new car is created instead at the next time step:

$$(2)x^{2}(3)\cdots(v_{\max})x^{L-v_{\max}(v_{\max}+1)} \quad \text{for } t=v_{\max}+1.$$

Here, $\Delta v=1$ and the space between the cars grows as $\Delta v t = t$. After $v_{\max}-2$ time steps, we finally get

$$\cdots(v_{\max})x^{v_{\max}}(v_{\max})\cdots(v_{\max})x^{L-v_{\max}(2v_{\max}-1)} \quad \text{for } t=2v_{\max}-1.$$

If one proceeds, it can be clearly seen that there are three scenarios ($m=0,1,2,\ldots$): The car created at site $i=0$ and $t=n$ (a) is deleted according to the left boundary conditions if $n=v_{\max}+3m$. (b) has $v_{\max}$ empty sites in front if $n=v_{\max}+1+3m$. (c) has $2(v_{\max}-1)$ empty sites in front if $n=v_{\max}+2+3m$. In other words, a self-repeating pattern establishes itself after a while according to

$$(2) \quad x^{2}\cdots(v_{\max})x^{2(v_{\max}-1)}(v_{\max})x^{v_{\max}}(v_{\max})x^{2(v_{\max}-1)}(v_{\max})x^{v_{\max}}(v_{\max})x^{2(v_{\max}-1)}\cdots,$$
$$(1) \quad x^{1}\cdots(v_{\max})x^{2(v_{\max}-1)}(v_{\max})x^{v_{\max}}(v_{\max})x^{2(v_{\max}-1)}(v_{\max})x^{v_{\max}}(v_{\max})x^{2(v_{\max}-1)}\cdots,$$
$$(0) \quad (2) \quad x^{2}\cdots(v_{\max})x^{2(v_{\max}-1)}(v_{\max})x^{v_{\max}}(v_{\max})x^{2(v_{\max}-1)}(v_{\max})x^{v_{\max}}(v_{\max})x^{2(v_{\max}-1)}\cdots.$$

This is perhaps astonishing because we naively would expect $v_{\max}$ unoccupied sites between two neighboring cars for $\alpha=1$. Actually, there are also spaces consisting of $2(v_{\max}-1)$ sites, which is a consequence of the hindrance that the injected cars feel from the front car at the beginning of the system. In other words, $v_{\max}-2$ additional sites—so-called ''buffers'' (the motivation for this name will be explained later)—occur, playing an important role for systems with maximum velocity $v_{\max} \geqslant 3$, as we will see below.

Besides, our reflections clearly show that one has to wait for at least $t=v_{\max}$ time steps until the self-repeating pattern is established. Within this time period the first car created at $t=0$ has moved onto site $i=v_{\max}^2$. Therefore, our considerations are only valid for systems whose size is much larger than $v_{\max}^2$, otherwise boundary effects must be taken into account.

From the self-repeating pattern it follows that the distance between two neighboring cars driving with $v_{\max}$ is alternately $d_1=v_{\max}$ and $d_2=2(v_{\max}-1)$, i.e.,

$$\begin{aligned} &d_1=2,\ d_2=2 \quad \text{for } v_{\max}=2,\\ &d_1=3,\ d_2=4 \quad \text{for } v_{\max}=3,\\ &d_1=4,\ d_2=6 \quad \text{for } v_{\max}=4,\\ &d_1=5,\ d_2=8 \quad \text{for } v_{\max}=5,\\ &d_1=6,\ d_2=10 \quad \text{for } v_{\max}=6,\\ &\qquad \cdots . \end{aligned}$$

That means that buffers occur only for $v_{\max}\geqslant 3$.

$v_{\max}=2$ is a special case behaving similarly to $v_{\max}=1$. It is therefore no surprise that the corresponding phase diagram, the global density, and the current resembles the case $v_{\max}=1$. If finite-size effects are left out of consideration, the current is obviously given by

$$q(\alpha=\beta=1,v_{\max}>1)=\tfrac{2}{3}$$

and the global density by

$$\overline{\rho}(\alpha=\beta=1,v_{\max}>1)=\frac{2}{3v_{\max}},$$

which coincides with numerical results.

We will now investigate the effect of the buffers for the extinction rate $\beta=1$. For that purpose, we consider a slightly smaller injection rate by working a ''disturbance'' in the $\alpha=\beta=1$ pattern, i.e., at each time step *except for one* a car is created at $i=0$. As the self-repeating pattern consists of three time steps, we have three possibilities to place the disturbance. In Appendix A the effect is illustrated with $v_{\max}\geqslant 5$ (in Appendixes A and B the notation $\hat{v}=v_{\max}$ is used). It turns out that the movement of the cars does not change at all for possibility (c). For (a) and (b), however, the disturbance influences the system for three time steps as three cars show a deviating behavior. Having a closer look at the sites affected by the disturbance, we see that the current $q_{\mathrm{dist}}(\beta=1,v_{\max}\geqslant 5)=\frac{3}{4}$ and the global density $\overline{\rho}_{\mathrm{dist}}(\beta=1,v_{\max}\geqslant 5)=3/4v_{\max}$ are higher there than for $\alpha=\beta=1$. As altogether $4v_{\max}$ sites are concerned by the disturbance, the effect increases with increasing $v_{\max}$.

Considering the site $i=0$, in Appendix A it is obvious that the effect of the disturbance is different for maximum velocities $v_{\max}<5$ as cars driving with $v_{\max}=4$ cannot be injected with $v=5$, cars driving with $v_{\max}=3$ cannot be injected with $v=4$, and so on. We do not go into details but just list the results: Placing a disturbance at the beginning of a system with $v_{\max}=2,3,4$, one gets

(a) $q_{\mathrm{dist}}(\beta=1,v_{\max}=4)=\frac{12}{17}$, $\overline{\rho}_{\mathrm{dist}}(\beta=1,v_{\max}=4)=\frac{3}{17}$,

$q_{\mathrm{dist}}(\beta=1,v_{\max}=3)=\frac{1}{2}$, $\overline{\rho}_{\mathrm{dist}}(\beta=1,v_{\max}=3)=\frac{1}{6}$,

$q_{\mathrm{dist}}(\beta=1,v_{\max}=2)=\frac{2}{5}$, $\overline{\rho}_{\mathrm{dist}}(\beta=1,v_{\max}=2)=\frac{1}{5}$;

(b) $q_{\mathrm{dist}}(\beta=1,v_{\max}=4)=\frac{3}{4}$, $\overline{\rho}_{\mathrm{dist}}(\beta=1,v_{\max}=4)=\frac{3}{16}$,

no effect of disturbance for $v_{\max}=3$,

$q_{\mathrm{dist}}(\beta=1,v_{\max}=2)=\frac{1}{2}$, $\overline{\rho}_{\mathrm{dist}}(\beta=1,v_{\max}=2)=\frac{1}{4}$;

(c) no effect of disturbance for $v_{\max}=2,3,4$.

Superposition of possibilities (a), (b), and (c) leads to the result that the effect of the disturbance is weaker for $v_{\max}=4$ than for corresponding systems with $v_{\max}\geqslant 5$. For maximum velocities $v_{\max}=2,3$, the current and the global density decrease, which is why the maximum of the curves in Fig. 2(a) is at $\alpha=1$ if $v_{\max}\leqslant 3$.

As far as the position of the maximum of the current is concerned, we can only give a hand-waving argument: It is obvious from Appendix A that the disturbance affects the development of two buffers. On the other hand, it can be easily seen that for $\alpha=\beta=1$ a buffer is created every three time steps (and consequently, two buffers are created in six time steps). Therefore, the strongest effect is expected when the system is disturbed with the rate $(1-\alpha)=\frac{1}{6}$. If $(1-\alpha)$ becomes higher, the buffers being necessary for the increase in the current and the global density cannot develop. This may be the reason why the maximum for the curves in Fig. 2(a) with $v_{\max}>5$ is found at $\alpha\approx\frac{5}{6}$.

For the injection rate $\alpha=1$ the buffers have an even more dramatic effect, which can be observed at the end of the system. In analogy to $\beta=1$, we start with the special case $\alpha=\beta=1$. By simple analytic considerations it turns out that a self-repeating pattern

$$\begin{aligned} &\cdots x^{2(v_{\max}-1)}(v_{\max})x^{v_{\max}}(v_{\max})x^{2(v_{\max}-1)}(v_{\max})x^{v_{\max}}(v_{\max})x^{2(v_{\max}-1)}(v_{\max}),\\ &\cdots (v_{\max})x^{2(v_{\max}-1)}(v_{\max})x^{v_{\max}}(v_{\max})x^{2(v_{\max}-1)}(v_{\max})x^{v_{\max}}(v_{\max})x^{v_{\max}-1},\\ &\cdots (v_{\max})x^{v_{\max}}(v_{\max})x^{2(v_{\max}-1)}(v_{\max})x^{v_{\max}}(v_{\max})x^{2(v_{\max}-1)}(v_{\max})x^{v_{\max}}, \end{aligned}$$

establishes itself at the end of the system, too ($L\gg v_{\max}^2$). It is important to mention that—due to $\beta=1$—no blockage occurs at all at the right boundary and that the buffers reach the right boundary with the rate $\alpha_{\mathrm{buffer}}=\frac{1}{3}$. The introduction of a disturbance (i.e., the consideration of an extinction rate that is slightly smaller than $\beta=1$) means here to place a single blockage at the end of the system. According to the self-repeating pattern consisting of three time steps, we have to-

consider three possibilities. From Appendix B it turns out the cars feel at the beginning of the system from the front car) play an important role at the end of the system, too. Here, they have the effect of a ''buffer'' against the influence of the right boundary. It can be seen from Appendix B that two buffers are necessary to neutralize the blockage effect at the end of the system. Therefore, as long as $(1-\beta)<\frac{1}{2}\alpha_{\text{buffer}}=\frac{1}{6}$, a jamming wave cannot develop.

For $\beta_c=\frac{5}{6}$, however, there is a jump in the global density (remember that our analytical considerations are based on systems with size $L\to\infty$; for $L=1024$ the change from free flow to traffic is less abrupt due to finite-size effects). As mentioned above, we have $\overline{\rho}(\alpha=1,\beta>\beta_c,\ v_{\max}\geqslant 5)=2/3v_{\max}$ in the free-flow regime and $\overline{\rho}(\alpha=1,\beta>\beta_c,\ v_{\max}\geqslant 5)=1-0.8\beta$ in the jamming regime. At $\beta_c=\frac{5}{6}$, $\overline{\rho}$ immediately increases from $2/3v_{\max}$ (free flow) to $\frac{1}{3}$ (jamming). That means that there is a jump of $(v_{\max}-2)/3v_{\max}$ at the critical extinction rate, which corresponds to the buffer density in the free-flow regime. In other words, at $\beta_c=\frac{5}{6}$ the buffers cannot neutralize the blockage at the right boundary any longer. The buffer effect breaks down, jamming waves propagate from the end of the system to the left, and the buffers ($v_{\max}-2$ sites on $3v_{\max}$ sites each) are completely occupied by cars. Consequently, both current and global density show similar behavior as the corresponding quantities for $v_{\max}=1$ if $\beta<\frac{5}{6}$.

Another interesting feature observed in Figs. 2(b) and 2(c) is that current and global density do not depend on the right (left) boundary conditions, i.e., not on $\beta$ (not on $\alpha$ and $v_{\max}$), if the system is in the free-flow (jamming) regime. This is not only valid for $\alpha=1$, but also for general injection and extinction rates, as can be seen in Fig. 3(a) for the current and for Fig. 3(b) for the global density.

In order to compare our results with those for corresponding systems with periodic boundary conditions we investigate the case $\beta=1-\alpha$. For $\beta=1-\alpha$, there are rather similar conditions at the left and at the right boundary and therefore systems with open and with periodic boundary conditions can be compared at best with each other.

The fundamental diagram for systems with periodic boundary conditions (PBC) is completely determined by the maximum velocity $v_{\max}$ (see [34] and references therein). The current of the system is given by $q^{\text{PBC}}(\rho<\rho_c)=v_{\max}\rho$ for freely moving and by $q^{\text{PBC}}(\rho>\rho_c)=1-\rho$ for jammed cars. The critical density is given by $\rho_c=1/v_{\max}+1$.

In the case of open boundary conditions, on the other hand, it turns out from numerical results for $v_{\max}\geqslant 5$ that the current in the free-flow (jamming) regime only depends on the injection (extinction) rate according to

$$q(\beta=1-\alpha)=\alpha \quad \text{for} \quad \alpha\leqslant\alpha_c,\beta\geqslant\beta_c,$$

$$q(\beta=1-\alpha)=0.8\beta \quad \text{for} \quad \alpha\geqslant\alpha_c,\beta\leqslant\beta_c,$$

and consequently the transition takes place at $\alpha_c=0.44$ ($\beta_c=0.56$). The global density for $\beta=1-\alpha$ shows finite-size effects as in the case $\alpha=1$. For large $L$, however, the transition from free flow to jamming becomes sharp. Then the global density is described by

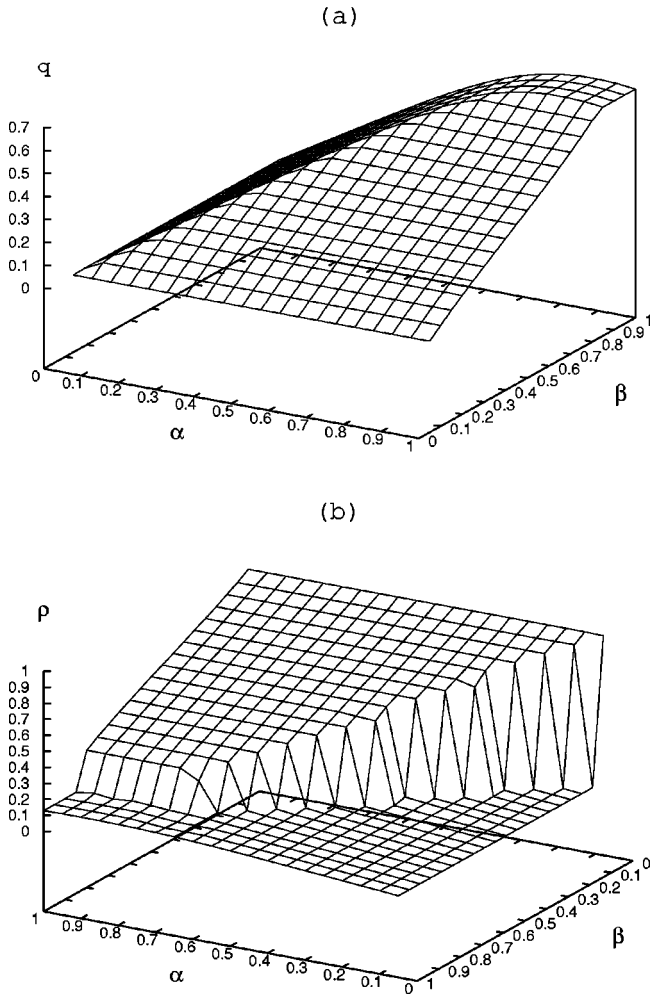


FIG. 3. (a) Current in dependence on the injection rate $\alpha$ and the extinction rate $\beta$ ($v_{\max}=5$). (b) Global density in dependence on the injection rate $\alpha$ and the extinction rate $\beta$ ($v_{\max}=5$).

$$\overline{\rho}(\beta=1-\alpha)=\frac{\alpha}{v_{\max}} \quad \text{for} \quad \alpha<\alpha_c,\beta>\beta_c,$$

$$\overline{\rho}(\beta=1-\alpha)=1-0.8\beta \quad \text{for} \quad \alpha>\alpha_c,\beta<\beta_c$$

with a jump at $\alpha_c=\frac{4}{9}\approx 0.44$ ($\beta_c=\frac{5}{9}\approx 0.56$).

The results for $\beta=1-\alpha$ induce the identity

$$q(\beta=1-\alpha)=q(\beta=1) \quad \text{for} \quad \alpha<\alpha_c,\beta>\beta_c,$$

$$q(\beta=1-\alpha)=q(\alpha=1) \quad \text{for} \quad \alpha>\alpha_c,\beta<\beta_c.$$

This indicates that the movement of the vehicles in the high-density or jamming regime is dominated by the right boundary conditions, and in the low-density or free-flow regime by the left boundary conditions. To get better insight into this question, we will have a closer look at the density profiles and the short-range correlation functions which are analyzed due to the following three special cases [see also Fig. 1(d)]. (i) $\beta=1$: shows the influence of the left boundary; (ii) $\alpha=1$: shows the influence of the right boundary; (iii) $\beta=1-\alpha$: systems with open and periodic boundary conditions can be compared at best with each other.

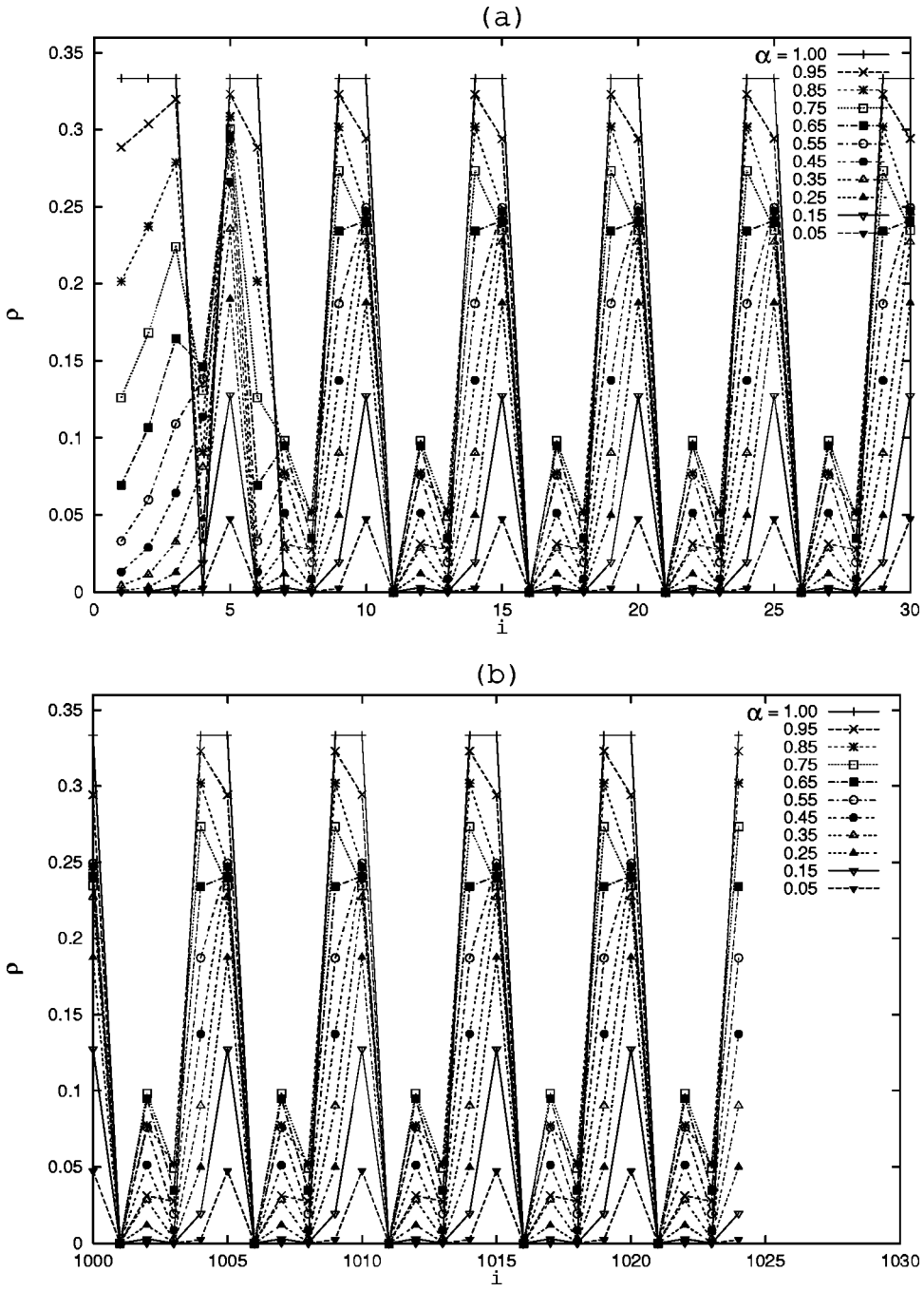


FIG. 4. (a) Density profiles at the beginning of the system ($\beta=1$). (b) Density profiles at the end of the system ($\beta=1$).

The investigations of this section clearly show that the case $v_{\max}=5$ includes all features which are characteristic for higher maximum velocities, too. For this reason we confine ourselves to systems with $v_{\max}=5$ (and $L=1024$) in the following.

## IV. DENSITY PROFILES

### A. $\beta=1$

In this section we investigate the influence of the left boundary on the density profiles. The best way to do this is to set $\beta=1$, because in that case the right boundary has no influence on the system.

From Figs. 4(a) and 4(b) it can be seen that the density profiles are characterized by a periodic structure. This is a significant difference from the case $v_{\max}=1$, where oscillations cannot be found at all [23]. For $v_{\max}=5$, however, the density profiles show a certain pattern recurring with the period $\Delta i=5$. In order to understand this phenomenon we consider the density profiles for very low injection rates first.

For $\alpha=0.05$ [see Figs. 4(a) and 4(b)] the probability of generating a car at $i=0$ in two successive time steps is very small and, therefore, the cars at the beginning of the system do not interact with each other. That means that a car which is created on $i=0$ with velocity 5 (according to the left boundary conditions) moves to $i=5$ at the next time step and can be found on the site $i=5n$ after $n$ time steps ($n=1,2,3,\ldots$). The density on these sites is $\rho\approx\alpha$. As it is obvious from Figs. 4(a) and 4(b), a car can also be found on $i=5n+4$ for small $\alpha$, too, but the probability for that is very small.

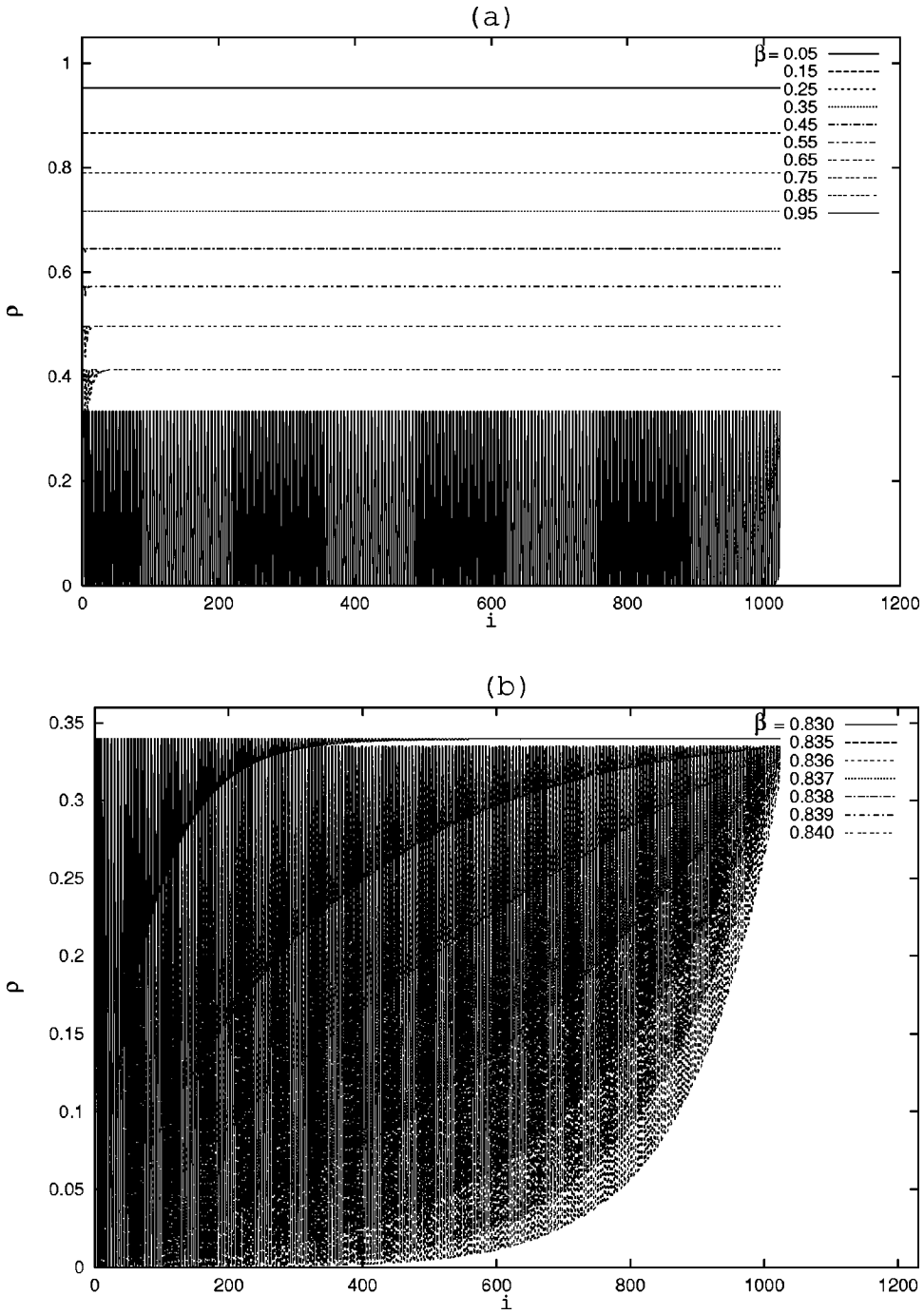


FIG. 5. (a) Density profiles for $\alpha=1$. (b) Density profiles for $\alpha=1$ around the critical extinction rate $\beta_c$. (c) Detail from (b) at the beginning of the system ($\alpha=1$). (d) Detail from (b) at the end of the system ($\alpha=1$).

For increasing injection rates $\alpha$, however, the probability of generating cars in two successive time steps increases and with it the hindrance that a car at the beginning of the system feels from the front car. This can be understood as follows: Let us create a car $A$ at time step $t$ and a car $B$ at time step $t+1$. Considering the system at $t+1$, we see that car $A$ is on $i=5$ having the velocity 5 whereas car $B$ on $i=0$ has the velocity 4 because there are only four empty sites to car $A$. At the time step $t+n$, car $A$ is on $i=5n$ and car $B$ is on $i=5(n-1)-1$. To sum it up, it can be said that the hindrance due to the left boundary conditions leads to a shift of the position of the cars within the system. This shift is reflected in the periodic pattern of Figs. 4(a) and 4(b). Whereas it is rather probable to find a car on $i=5n+5$ and on $i=5n+4$, the probability of finding a car on $i=5n+2$ is much smaller and for $i=5n+3$ it nearly vanishes.

The most important result, however, is the fact that the sites $i=6+5n$ are *never* occupied according to the left boundary conditions so that the density on these sites has the value $\rho(i=6+5n)=0$ for all $\alpha$. Before turning back to this point, we have to look at the case $\alpha=\beta=1$, which is of

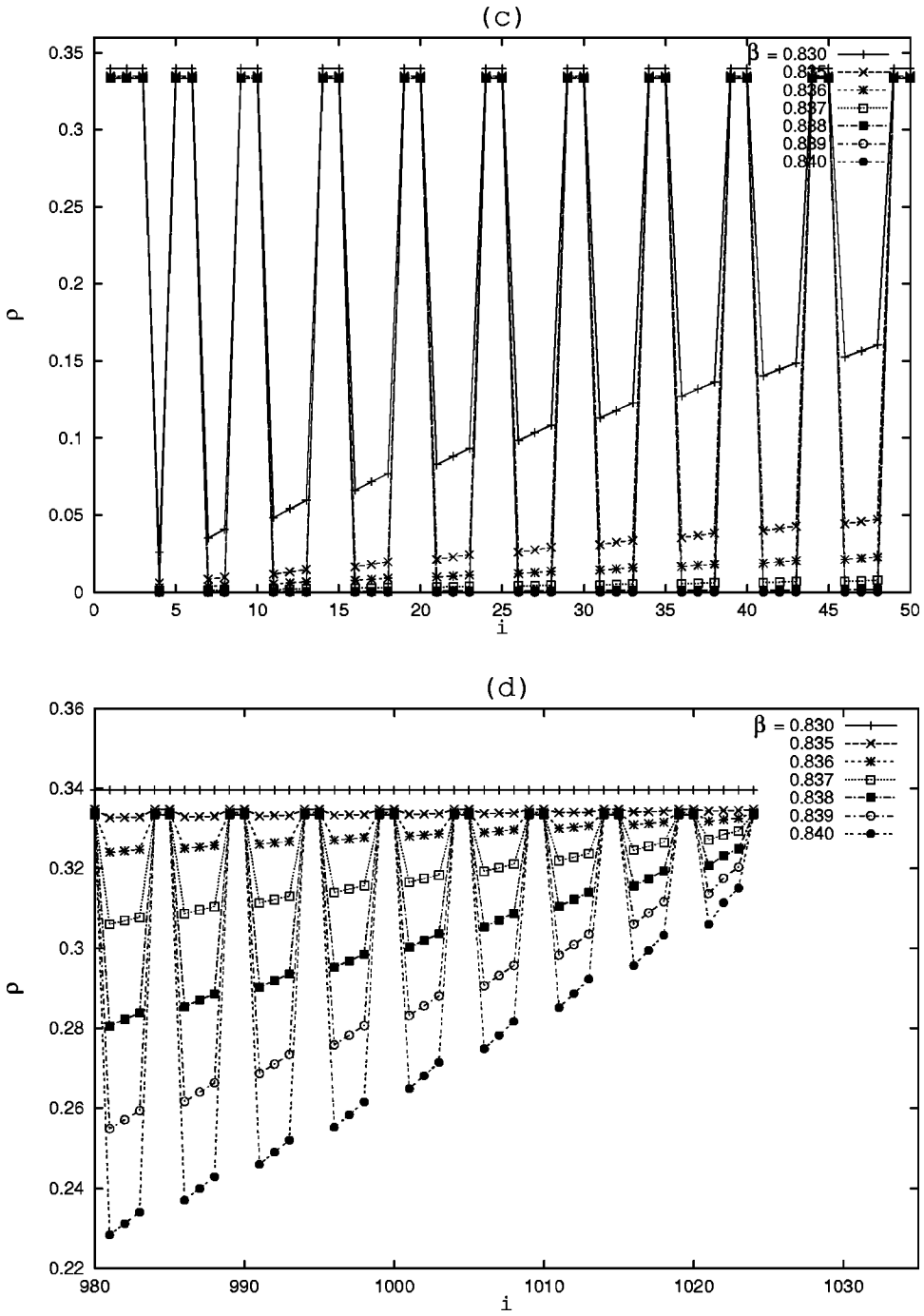


FIG. 5. (*Continued*).

special interest in the following section, too.

For $\alpha=\beta=1$, the corresponding density profile has the following form:

$$\rho(i)=\tfrac{1}{3} \quad \text{if } i=5n+4 \text{ or } i=5n+5,$$

$$\rho(i)=0 \quad \text{otherwise,}$$

as can be easily deduced from the left boundary conditions.

### B. $\alpha=1$

We investigate the influence of the right boundary now. Unfortunately, the influence of the left boundary cannot be completely left out of consideration by setting, for example, $\alpha=0$, because in that case no cars would be generated at all. Instead, we choose $\alpha=1$, because only for $\alpha=1$ are the cars deterministically created. This allows us to distinguish between the influence of the right and of the left boundary.

In Fig. 5(a), we can see that the situation for $\alpha=1$ is very different from that described in the preceding section. For high extinction rates we still recognize the periodic structure already known from the case $\beta=1$. For extinction rates $\beta$ between 0.75 and 0.85, something interesting happens: the oscillations vanish and the envelope of the density profile rises. For low extinction rates, the density profiles are just a constant whose value increases with decreasing $\beta$.

In order to understand this change, we consider density profiles for $0.83\leqslant\beta\leqslant0.84$ in Figs. 5(b)–5(d). On $i=4+5n$

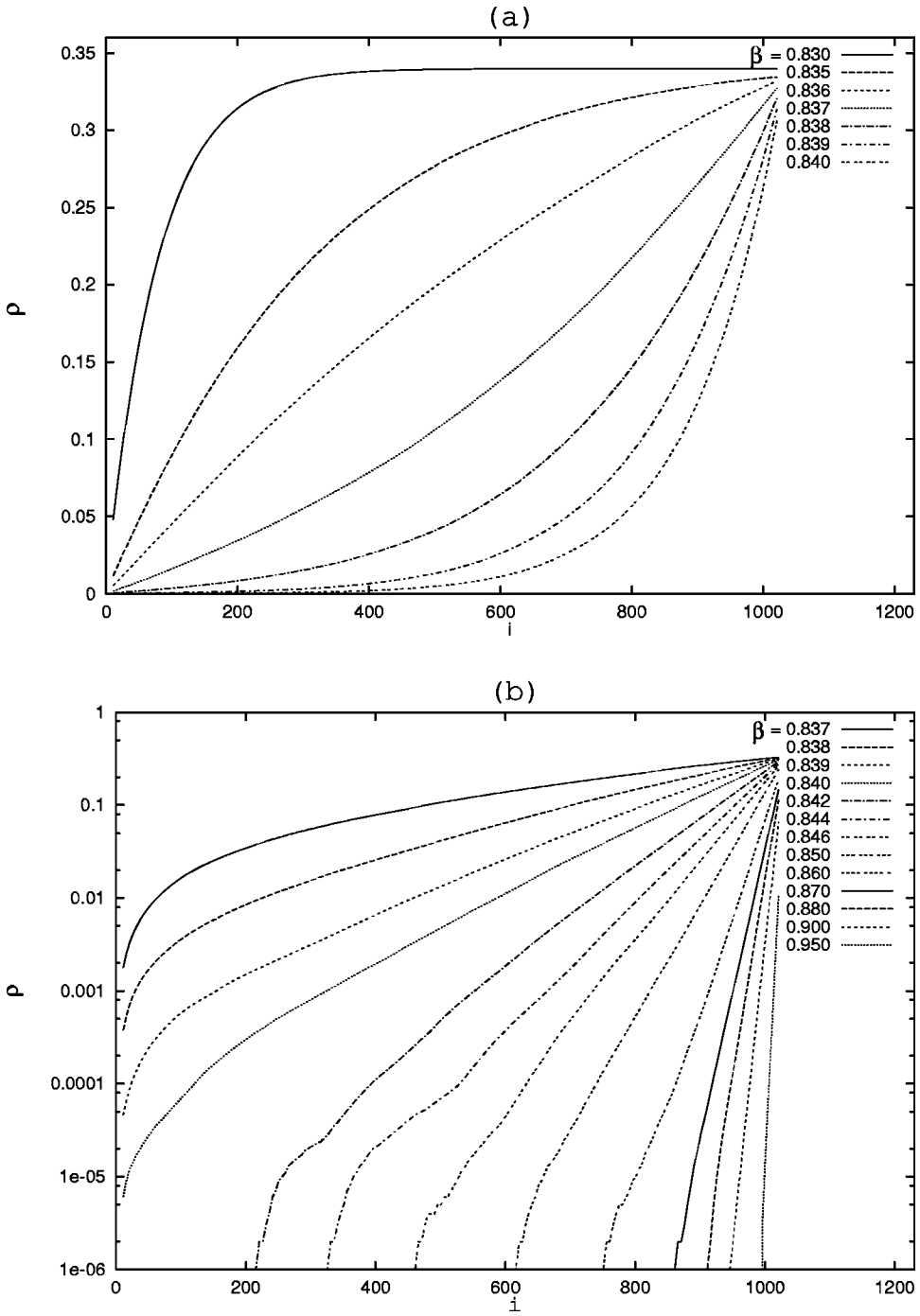


FIG. 6. (a) Density profiles from (b) taking only the sites $i=6+5n$ into account ($\alpha=1$). (b) Logarithmic plot of the density profiles for $\beta>\beta_c$ taking only the sites $i=6+5n$ into account ($\alpha=1$). (c) Logarithmic plot of $\rho_{\max}-\rho(i=6+5n)$ for $\alpha=1$. (d) Gradient of the density profiles in (b) and (c) depending on the extinction rate $\beta$ ($\alpha=1$). (e) Maximum value of the density profiles $\rho(i=6+5n)$ on $i=1021$ ($\alpha=1$).

and $i=5+5n$ we find $\rho(i)=\frac{1}{3}$ resulting from the influence of the left boundary (see Sec. IV A). The other sites (with $\rho=0$ for $\beta=1$), however, increasingly reflect the influence of the right boundary with decreasing extinction rates. Coming from high $\beta$, the density on $i=6+5n$, $i=7+5n$, and $i=8+5n$ seems to ''come away'' from the $\rho(i)=0$ line starting at the right boundary. This phenomenon can be explained due to the repulsion the car feels at the right boundary with decreasing probability $\beta$ of being extinct. Consequently, a jam develops at the right boundary which expands to the left. For $\beta\approx0.837$, the influence of the right boundary finally reaches the beginning of the system [Fig. 5(c)]. For $\beta=0.84$, the sites $i=4+5n$ and $i=5+5n$ indicate the repulsion at the right boundary, too, as the density profile becomes $\rho>\frac{1}{3}$ there. In parallel to this, the oscillations resulting from the left boundary conditions vanish, a process which starts from the end of the system as well.

Our observations have been quite qualitative so far. In the

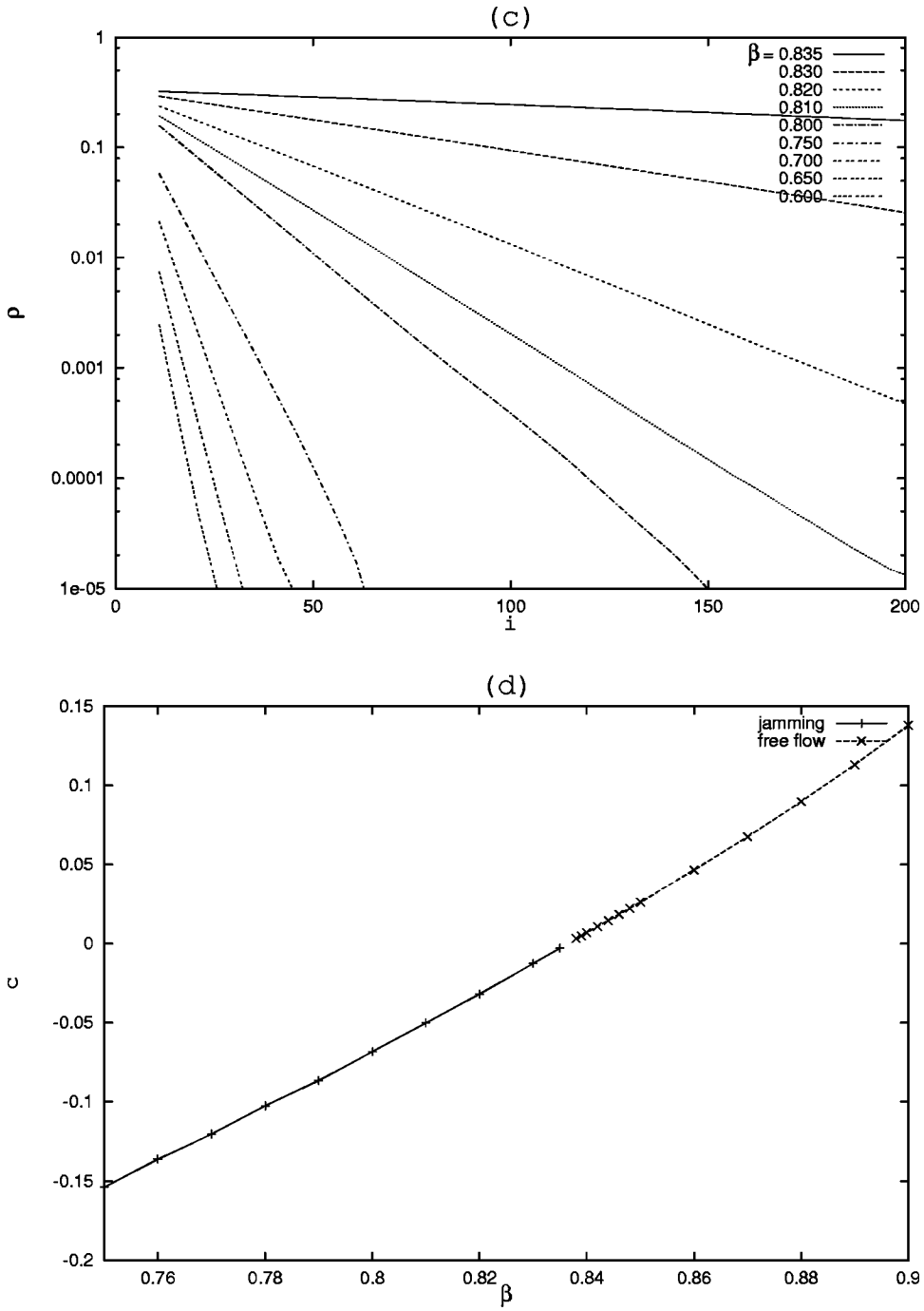


FIG. 6. (*Continued).*

following the transition described above will be analyzed in detail and for that purpose we will have a closer look at the sites $i=6+5n$. As we know from the preceding section, these sites are never occupied according to the left boundary conditions. In other words, the occupation of the sites $i=6+5n$ is *exclusively* an effect of the right boundary. Therefore, these sites play an important role as they show the repercussion of the right boundary on the system.

The density on these sites is shown in Figs. 6(a)–6(c). The density profiles correspond to the same $\beta$ as in Fig. 5(b), but here all sites except for $i=6+5n$ are left out of consideration. Let us first consider the density profiles for $\beta>\beta_c$ [Fig. 6(b)], which are exponential functions $\rho$ (i=6+5n) $=\rho_{\max}(\beta)e^{c(\beta)(i-L)}$ [$\rho_{\max}(\beta)$ is the maximum value of the density on the sites $i=6+5n$]. In Fig. 6(d) the exponent $c(\beta)$ is drawn against the extinction rate $\beta$ and it is obvious that $c(\beta)=k(\beta-\beta_c)$ with $\beta_c=0.8362$ and $k\approx 2$. Whereas $\beta_c$ can be clearly identified as the critical extinction rate where the transition from freely moving to jammed traffic takes place, the factor $k$ is still an open question.

If we pass over to the density profiles for $\beta<\beta_c$, it can be easily seen in Figs. 6(c) and 6(d) that the density profiles have the form $\rho(i=6+5n)=\rho_{\max}(\beta)[1-e^{c(\beta)i}]$.

The behavior of the density profiles described in this sec tion has the following physical explanation. As is well known, the right boundary has no effect on the density pro-

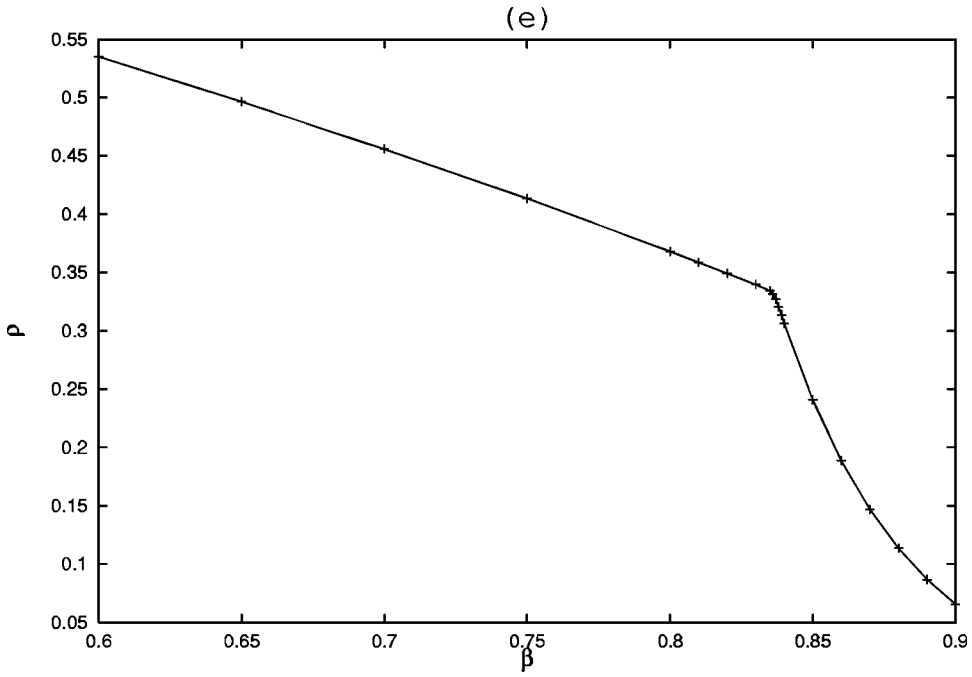


FIG. 6. (*Continued).*

files for $\beta=1$. With decreasing $\beta$, however, there is a growing probability of a blockage at the end of the system, i.e., cars are increasingly hindered from moving out of the system. Consequently, a jam develops showing the growing influence of the right boundary with decreasing $\beta$. For $\beta>\beta_c$, the influence of the right boundary diminishes exponentially [Fig. 6(b)]. Figure 6(a) further shows that the left boundary conditions are still valid for the whole system, which can be seen at the oscillations of the density profile and in the constant value $\rho\ (i)=\frac{1}{3}$ on the sites $i=4+5n$ and $i=5+5n$ characteristic for the case $\alpha=\beta=1$. For decreasing $\beta$, the jam and with it the influence of the right boundary expand to the left.

At $\beta=\beta_c$, the repercussion of the right boundary reaches the left boundary, and the decay of the jam is proportional to $i$. Simultaneously, the influence of the left boundary is still-present in the whole system, too, which manifests itself in the oscillations in the density profile going from the left to the right boundary [Fig. 6(a)]. So it can be said that for the extinction rate $\beta=\beta_c$, the influences of the left and right boundary coexist in the whole system.

However, beginning from the right, the oscillations vanish when the extinction rate is further decreased [Fig. 6(a)]. This indicates that the influence of the left boundary is pushed back for $\beta<\beta_c$. The form $\rho(i=6+5n)=\rho_{\max}(\beta)[1-e^{c(\beta)i}]$ shows the decrease of unoccupied sites and may suggest a symmetry around the transition point.

For very small $\beta$, the left boundary does not have any relevance at all for the movement of the cars in the bulk.

Finally, let us address the maximum value $\rho_{\max}(\beta)=\max[\rho(i=6+5n)]$. From Fig. 6(a) it is obvious that $\rho_{\max}(\beta)$ can be identified with the density on site $i=1021$, $\rho_{\max}(\beta)=\rho\ (\beta,\ i=1021)$. From Fig. 6(e) it turns out then that

$$\rho_{\max}(\beta)=\rho_{\max}(\beta_c)e^{k_1(\beta-\beta_c)} \quad \text{for} \quad \beta>\beta_c,$$
$$\rho_{\max}(\beta)=1+k_2\beta \quad \text{for} \quad \beta<\beta_c$$

($k_1\approx-24.46$; $k_2\approx-0.8$; $\beta_c=0.8362$). Thus, the transition from freely moving to jammed traffic is reflected at the right boundary, too.

### C. $\beta=1-\alpha$

We have already mentioned that for $\beta=1-\alpha$ we have rather similar conditions at the left and, at the right boundary and, therefore, systems with open and with periodic boundary conditions can be compared at best with each other in that case.

We must keep in mind, however, that there are significant differences for $\beta=1-\alpha$, too, especially if the randomization probability is $p=0$: In systems with periodic boundary conditions, the movement of the cars is fully deterministic and the car density $\rho$ in the system remains constant. Each site in the system has the same probability of being occupied and, therefore, the density profiles of systems with periodic boundary conditions are constants with the value $\rho$ (the latter statement is also valid for randomization probabilities $p>0$). For corresponding systems with open boundary conditions—due to the injection rate $\alpha$ and the extinction rate $\beta$—we always have a nondeterministic element at the boundaries of the system, as well as for the randomization probability $p=0$ (which only refers to the movement in the bulk).

Generally speaking, the density profiles for $\beta=1-\alpha$ show a similar behavior to those for the case $\alpha=1$ (see Fig. 7): For very low extinction rates (and high injection rates), the density profiles are identical with the density profile of a corresponding system with periodic boundary conditions. For high $\beta$ (and low $\alpha$) the density profiles show the periodic structure already known from the previous sections as a typical feature of the free-flow regime. At $\beta_c=0.56$ (and $\alpha_c=0.44$), the transition from free flow to jamming takes place. For $\beta>\beta_c$, the curves have the form $\rho\ (i=6+5n)=\rho_{\max}(\beta)e^{c(\beta)(i-L)}$, for $\beta<\beta_c$ $\rho$(i=6+5n)=$\rho$max($\beta$)[1

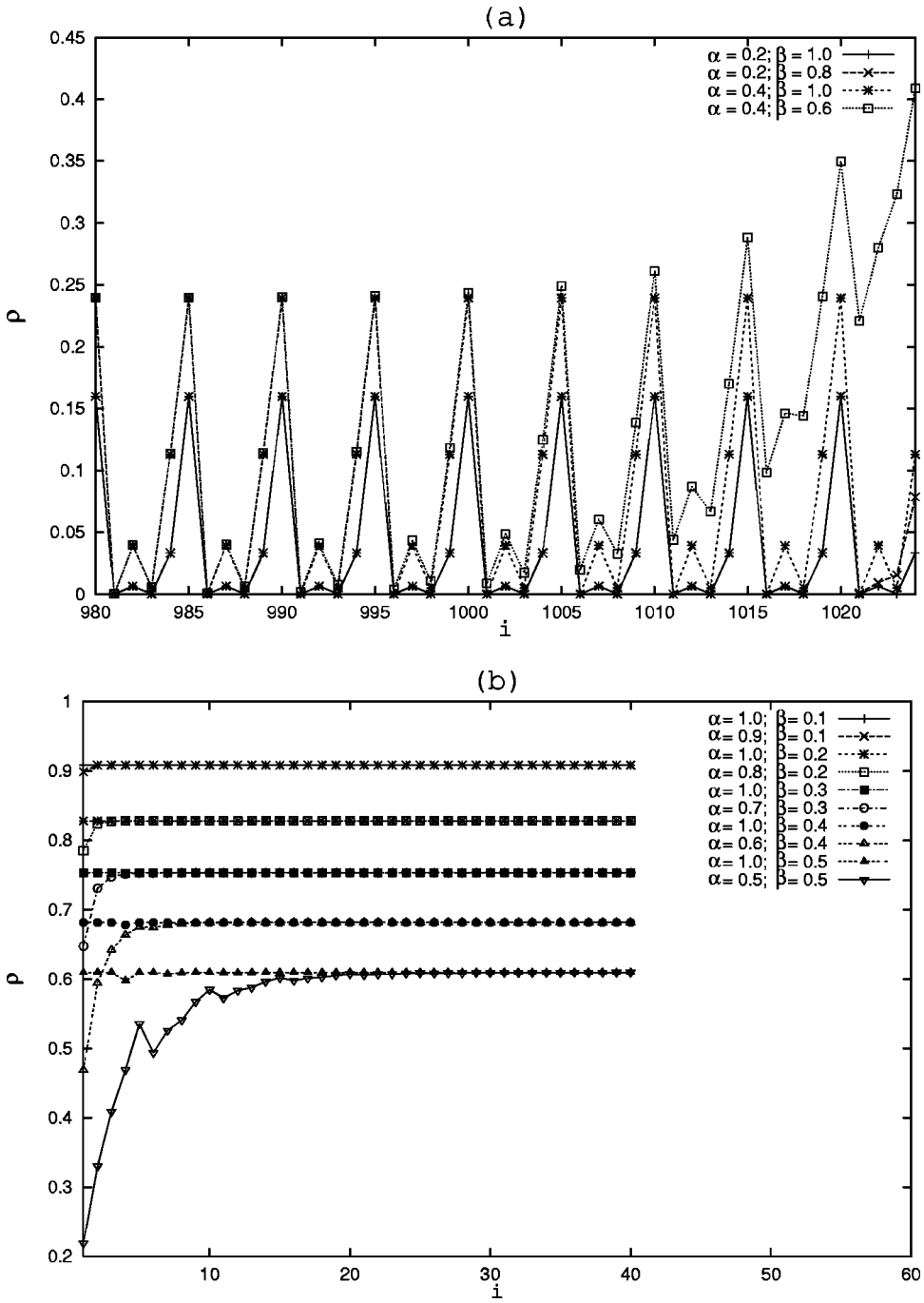


FIG. 7. (a) Comparison of the density profiles for $\beta=1-\alpha$ and $\beta=1$. (b) Comparison of the density profiles for $\beta=1-\alpha$ and $\alpha=1$.

$-e^{c(\beta)i}$] and for $\beta=\beta_c$ we have a straight line. The only difference from the $\alpha=1$ case is the value of the critical extinction rate and of $k$: For $\beta=1-\alpha$ we have $\beta_c=0.56$ and $k=3.75$.

In Sec. III we have already mentioned that in the high-density regime the global density (current) for $\beta=1-\alpha$ is identical with the global density (current) for $\alpha=1$ and in the low-density regime with the global density (current) for $\beta=1$. From Figs. 8(a) and 8(b) it is obvious that similar effects can also be observed for the density profiles, too. Having a closer look at them, we see that the profiles for $\beta=1-\alpha$ and $\beta=1$ are identical if the injection rate $\alpha$ is low. For increasing $\alpha$, the density profiles for $\beta=1-\alpha$ start to lift at the end of the system, indicating the growing influence of the right boundary on the system for increasing $\alpha$. On the other hand, comparing the density profiles for $\beta=1-\alpha$ and $\alpha=1$ with each other, we see that they are identical for very low $\beta$. For increasing $\beta$, the density profile ''drops'' at the beginning of the system. Accordingly, this behavior shows the growing influence of the left boundary on the system. In the transition regime, however, the density profiles for $\beta=1-\alpha$ are very different from those for the cases $\alpha=1$ and $\beta=1$.

## V. CORRELATION FUNCTIONS

In this section we consider correlation functions

$$C(i,t)=\langle \eta(i',t'),\eta(i'+i,t'+t)\rangle_{i',t'}-\rho^2$$

for short ranges with

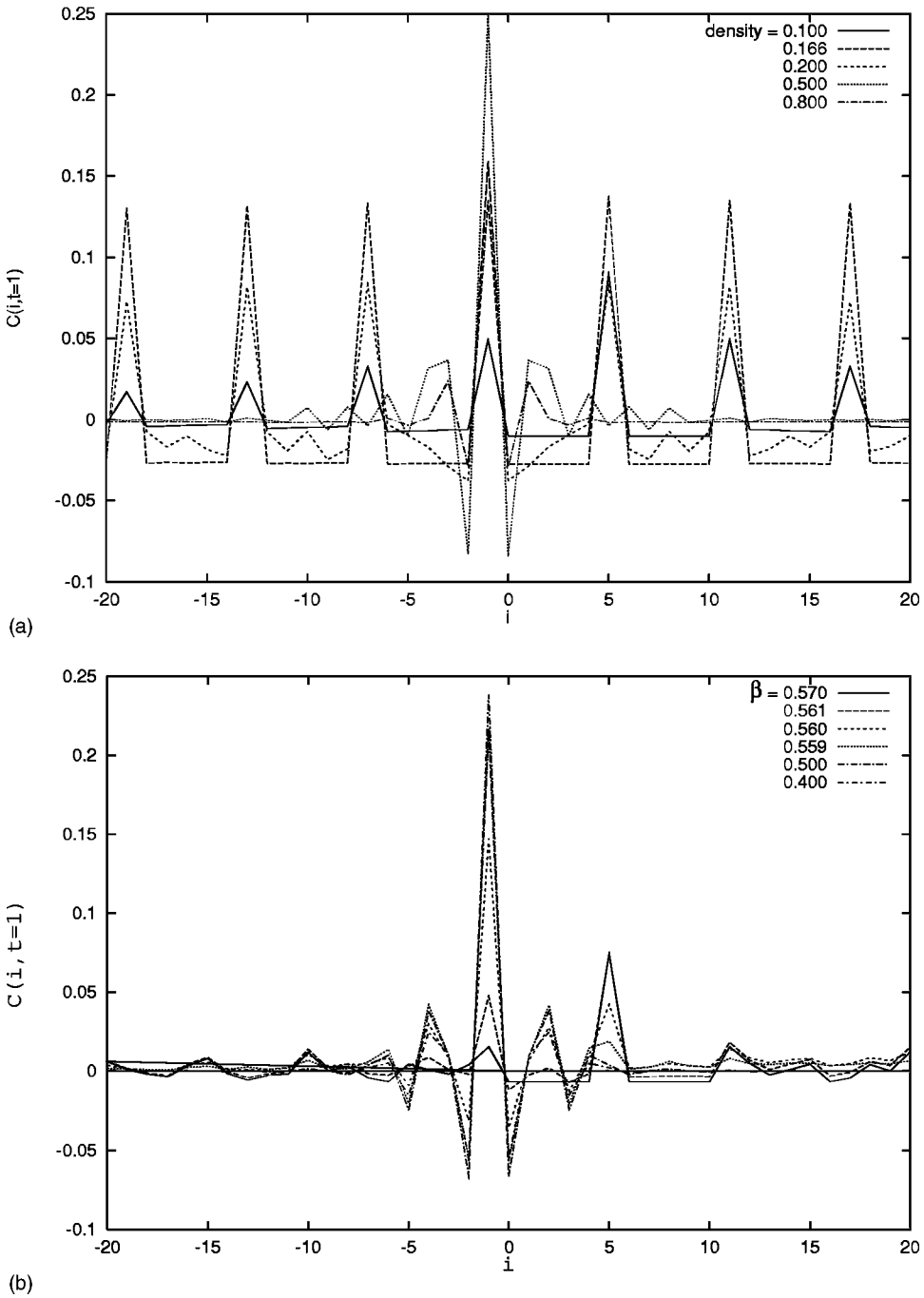


FIG. 8. (a) Correlation functions for systems with periodic boundary conditions. (b) Correlation functions in the middle of the system for $\beta=1-\alpha$. (c) Correlation functions at the beginning of the system for $\beta=1-\alpha$. (d) Correlation functions at the end of the system for $\beta=1-\alpha$.

$$\eta(i',t')=1 \quad \text{if site } i' \text{ is occupied at time } t',$$
$$\eta(i',t')=0 \quad \text{otherwise.}$$

This kind of correlation function has already been investigated for systems with periodic boundary conditions and the randomization probability $p=0.5$ in [28]. It turned out that in the free-flow regime there is a propagating peak at $i=v_{\max}t$ with a shoulder at $i=v_{\max}t-1$ and with anticorrelations around it. The density where these anticorrelations are maximally developed is defined as the density where the transition from free flow to jamming takes place. For higher densities, a jamming peak occurs at $i=-1$ [28].

It would be interesting to see if these features can also be found for systems with open boundary conditions. But considering the deterministic case in this paper, we should investigate the correlation functions for systems with periodic boundaries and $p=0$ first. From Fig. 8(a), it can be seen that the propagating peak is sharp and that there are further peaks at $i=v_{\max}t\pm 6n(n=1,2,\ldots)$ as the movement of the cars in the ring is deterministic. Due to the fact that the initial configuration is random, however, these peaks become smaller and smaller with increasing $n$. Between the peaks, anticorrelations are observed which are best developed around the

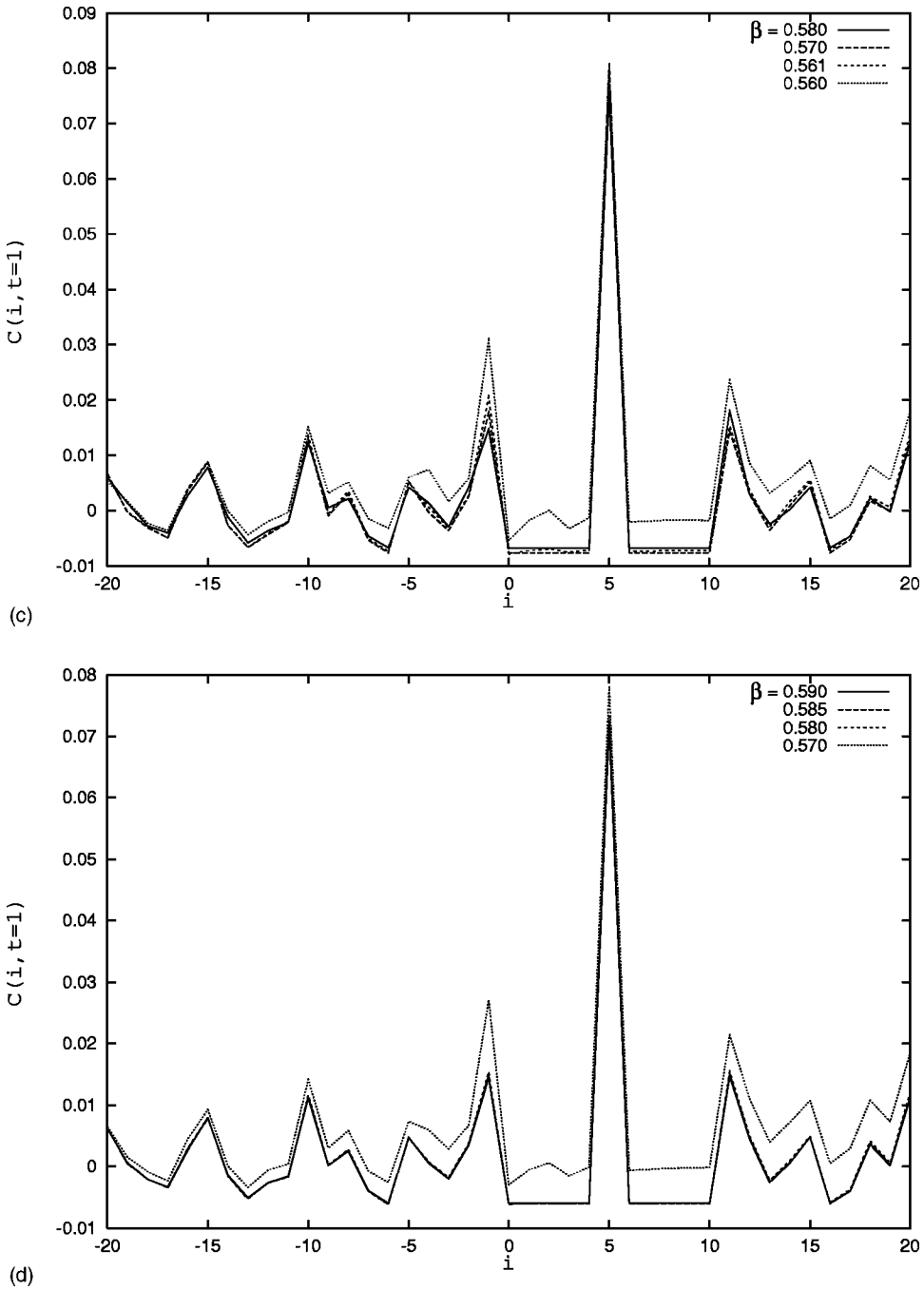


FIG. 8. (*Continued).*

peak at $i=v_{\max}t$. Generally speaking, it can be said that in the free-flow regime the correlation functions $C(i,t)$ are symmetric around the site $i=v_{\max}t$.

Coming from low densities, the anticorrelations become deeper and deeper with increasing $\rho$. At $\rho=\rho_c=1/(v_{\max}+1)$, the car distribution is well-defined: all vehicles drive with the maximum velocity $v_{\max}=5$, and between two neighboring cars there are $v_{\max}=5$ empty sites each. Correspondingly, the correlation function for $\rho=\rho_c$ is periodic with

$$C(i,t)=\rho-\rho^2 \quad \text{if} \quad i=v_{\max}t\pm 6n,$$

$$C(i,t)=-\rho^2 \quad \text{otherwise.}$$

At this density where the transition from free flow to jamming takes place, the anticorrelations reach their minimum.

For higher densities, a jamming peak develops at $i=-1$ (due to the hindrance that the back car feels in the jam) with anticorrelations at $i=\pm 1$. At all other sites, peaks and anticorrelations vanish. If the density further increases, fewer and fewer cars move (with $v>0$) and, therefore, the anticorrelations at $i=\pm 1$ disappear. Corresponding to the symmetry around $i=v_{\max}t$ in the free-flow regime, the correlation functions for $\rho>\rho_c$ are symmetric around $i=-1$.

Let us turn back to systems with open boundary conditions, which is the real topic of this paper. In Fig. 8(b), we consider correlation functions from the middle of the system

because the influence of the boundaries is minimal there. It is obvious that for high densities the correlation functions in systems with open boundary conditions are nearly identical. Merely the minor maxima at $i=\pm 2$ in Fig. 8(a) shift onto $i=\pm 3$ in Fig. 8(b).

If the density in the system is low, however, the situation is completely different: For systems with open boundaries, we have a random element at the boundaries where cars are randomly created and deleted at each time step. Therefore, due to the permanent presence of randomization, even if the movement in the bulk is deterministic, we can only observe the propagating at $i=v_{\max}t$ (and a very small one at $i=v_{\max}t\pm 6$). Around the propagating peak there are anticorrelations, too, but they are not so well-developed as the anticorrelations of the corresponding correlation function in the case of periodic boundary conditions. However, a common feature of systems with open and periodic boundary conditions is the symmetry of the correlation functions around $i=v_{\max}t$ in the free-flow regime.

As we have already mentioned, the anticorrelations around the propagating peak play an important role in systems with periodic boundary conditions, and we will now discuss the question if similar features can be observed for systems with open boundary conditions. In Figs. 8(b)–8(d) we consider short-range correlation functions at the beginning, the middle, and the end of the system. Coming from high extinction rates $\beta$ (with $\beta=1-\alpha$), the anticorrelations become deeper and deeper everywhere in the system. But what is interesting is the fact that the anticorrelations start to vanish again at an extinction rate where the influence of the right boundary reaches the corresponding sites (see also Sec. V C). Strictly speaking, the anticorrelations start to vanish at about $\beta=0.42$ (at the end), $\beta=0.43$ (in the middle), and $\beta=0.44$ (at the beginning).

Therefore, to sum up it can be said that the injection rate (extinction rate) where the probability to find a car in the neighborhood of another car is minimal (i.e., where the anticorrelations start to vanish) can be considered as the injection rate $\alpha_c$ (extinction rate $\beta_c$) where the transition from free flow to jamming takes place.

## VI. CONCLUSIONS AND DISCUSSION

Systems with open boundaries where cars move deterministically with maximum velocity $v_{\max}>1$ show interesting features mainly resulting from the competition of the left and right boundary for the influence in the system and from the existence of so-called ''buffers.''

The latter plays a fundamental role in the comparison of systems with $v_{\max}\geqslant 3$ and $v_{\max}=1$. One of the most important questions in this context is why the border between free flow and jamming for $v_{\max}\geqslant 3$ has such a different course from the corresponding border for the case $v_{\max}=1$. By simple analytical considerations it turns out that—as a consequence of the hindrance that an injected car feels from the front car—spaces $>v_{\max}$ develop for high injection rates $\alpha$ [for the special case of $\alpha=\beta=1$ there are alternately $2(v_{\max}-1)$ and $v_{\max}$ sites between neighboring cars for all $v_{\max}>1$]. That means in addition to the expected $v_{\max}$ sites, further sites occur that are the reason why the maximum current is found at $\alpha<1$ and $\frac{5}{6}\leqslant\beta\leqslant 1$ for $v_{\max}\geqslant 5$. We call these additional sites ''buffers'' because they also have a buffer effect at the end of the system: Due to the buffers, the development of jamming waves is suppressed up to an injection rate $\beta=\frac{5}{6}$ (for high $\alpha$ and $v_{\max}\geqslant 5$) and this buffer effect is responsible for the characteristic course of the free-flow–jamming border for $v_{\max}\geqslant 5$. The transition from the free flow to the congested phase is of first order and accompanied by the collapse of the buffers.

In this context, it should be emphasized that the occurrence of buffers—and consequently the specific features of the $v_{\max}\geqslant 3$ model—is due to the parallel updating mechanism and not an effect of the particular injection rule. Naturally, there are other possibilities of generalizing the ASEP to $v_{\max}>1$, for example one could keep the existence of the car at $i=0$ if $i=1$ is occupied by another car. Simulations based on this alternative rule show that the phase diagram and the $\alpha,\beta$ dependence of the current are qualitatively the same as the corresponding quantities considered in this paper. This has been confirmed by analytical investigations of the special case $v_{\max}=5$, $\alpha=\beta=1$ (according to Sec. III) where buffers occur, too.

As global density and current (from now on we refer again exclusively to the injection rule defined in Sec. II) show no qualitative differences for $v_{\max}\geqslant 5$, a detailed analysis of the influence of the boundary conditions on the system (by means of density profiles and short-range correlation functions) is confined to the maximum velocity $v_{\max}\geqslant 5$. Furthermore, our numerical investigations are based on systems with size $L=1024$. It must be mentioned here that finite-size effects occur which do not play an important role, however the discontinuous transition in the global density becomes continuous and the value for the critical extinction rate ($\beta_c=0.836$ for $\alpha=1$ and $L=1024$) is slightly higher than in the case $L\to\infty$.

If we consider a single site of the system, there are three possibilities: *A*, the site is exclusively under the influence of the left boundary; *B*, the site is exclusively under the influence of the right boundary; *C*, the site is under the influence of both the left and the right boundary. In the free-flow regime, the system consists of sites of the types *A* and *C*; in the jamming regime, the system consists of sites of the type *B* and *C*. The critical injection rate $\alpha_c$ (the critical extinction rate $\beta_c$), where the transition from freely moving to jammed traffic takes place, is the only $\alpha$ ($\beta$) where *all* sites of the system belong to the *C* type, i.e., where the influence of the left and of the right boundary coexists in the whole system. The farther we go away from the transition point, the stronger is the dominance of the *A* sites in the free-flow regime and of the *B* sites in the jamming region.

In the free-flow (jamming) regime the current does not depend on the injection rate $\alpha$ (extinction rate $\beta$), which confirms the dominance of the left (right) boundary influence in the free-flow (jamming) regime.

Comparing the density profiles for $v_{\max}=5$ with those for $v_{\max}=1$, we see that the most significant differences are found in the free-flow regime: In the free-flow regime, the density profile for $v_{\max}=5$ shows periodic structure with the period $\Delta i=v_{\max}=5$, which is due to the free movement of the cars. Another interesting result is the fact that the sites $i=6+5n$ $(n=1,2,\ldots)$ are never occupied when they are

beyond the sphere of influence of the right boundary. In the jamming regime, however, the density profiles for $v_{\max}=5$ and $v_{\max}=1$ are nearly the same. The investigation of the density profiles, especially the behavior on the sites $=6+5n$, enables the precise localization of the phase transition.

The short-range correlation functions $C(i,t)$ show that there are parallels between systems with open and with periodic boundary conditions, which are the following: In the free-flow regime, $C(i,t)$ is symmetric around the site $i=v_{\max}t$ and in the jamming region around $i=-1$, which may suggest a symmetry. Free flow (jamming) is characterized by a peak at $i=v_{\max}t(i=-1)$ with anticorrelations around it. Furthermore, in systems with open or periodic boundary conditions, the anticorrelations around the free-flow peak are maximally developed when the transition from free flow to jamming takes place.

## ACKNOWLEDGMENTS

This work was supported by the Land of North Rhine-Westphalia and by the OTKA (T029985).

## APPENDIX A: DISTURBANCE AT THE BEGINNING OF THE SYSTEM

(a)

$$\vdots \qquad\qquad \vdots$$

$$(2)\ x^3(3)x^5\cdots(\hat{v})x^{2(\hat{v}-1)}(\hat{v})x^{\hat{v}}(\hat{v})x^{2(\hat{v}-1)}(\hat{v})^{\hat{v}}(\hat{v})x^{2(\hat{v}-1)}(\hat{v})\cdots$$

$$(1)\ x^1(3)x^3\cdots(\hat{v})x^{2(\hat{v}-1)}(\hat{v})x^{\hat{v}}(\hat{v})x^{2(\hat{v}-1)}(\hat{v})^{\hat{v}}(\hat{v})x^{2(\hat{v}-1)}(\hat{v})\cdots$$

$$(0)\ (2)x^3(4)\cdots(\hat{v})x^{2(\hat{v}-1)}(\hat{v})x^{\hat{v}}(\hat{v})x^{2(\hat{v}-1)}(\hat{v})^{\hat{v}}(\hat{v})x^{2(\hat{v}-1)}(\hat{v})\cdots$$

$$(-)\ x^2(3)x^5\cdots(\hat{v})x^{2(\hat{v}-1)}(\hat{v})x^{\hat{v}}(\hat{v})x^{2(\hat{v}-1)}(\hat{v})^{\hat{v}}(\hat{v})x^{2(\hat{v}-1)}(\hat{v})\cdots \leftarrow \text{no car}$$

$$(5)\ x^5(4)x^7\cdots(\hat{v})x^{2(\hat{v}-1)}(\hat{v})x^{\hat{v}}(\hat{v})x^{2(\hat{v}-1)}(\hat{v})^{\hat{v}}(\hat{v})x^{2(\hat{v}-1)}(\hat{v})\cdots \qquad \text{injected!}$$

$$(4)\ x^4(4)x^4\cdots(\hat{v})x^{2(\hat{v}-1)}(\hat{v})x^{\hat{v}}(\hat{v})x^{2(\hat{v}-1)}(\hat{v})^{\hat{v}}(\hat{v})x^{2(\hat{v}-1)}(\hat{v})\cdots$$

$$(3)\ x^3(4)x^4\cdots(\hat{v})x^{2(\hat{v}-1)}(\hat{v})x^{\hat{v}}(\hat{v})x^{2(\hat{v}-1)}(\hat{v})^{\hat{v}}(\hat{v})x^{2(\hat{v}-1)}(\hat{v})\cdots$$

$$(2)\ x^2(4)x^4\cdots(\hat{v})x^{2(\hat{v}-1)}(\hat{v})x^{\hat{v}}(\hat{v})x^{2(\hat{v}-1)}(\hat{v})^{\hat{v}}(\hat{v})x^{2(\hat{v}-1)}(\hat{v})\cdots$$

$$(1)\ x^1(3)x^4\cdots(\hat{v})x^{2(\hat{v}-1)}(\hat{v})x^{\hat{v}}(\hat{v})x^{2(\hat{v}-1)}(\hat{v})^{\hat{v}}(\hat{v})x^{2(\hat{v}-1)}(\hat{v})\cdots$$

$$(0)\ (2)x^3(4)\cdots(\hat{v})x^{2(\hat{v}-1)}(\hat{v})x^{\hat{v}}(\hat{v})x^{2(\hat{v}-1)}(\hat{v})^{\hat{v}}(\hat{v})x^{2(\hat{v}-1)}(\hat{v})\cdots$$

$$(2)\ x^2(3)x^5\cdots(\hat{v})x^{2(\hat{v}-1)}(\hat{v})x^{\hat{v}}(\hat{v})x^{2(\hat{v}-1)}(\hat{v})^{\hat{v}}(\hat{v})x^{2(\hat{v}-1)}(\hat{v})\cdots$$

$$(1)\ x^1(3)x^3\cdots(\hat{v})x^{2(\hat{v}-1)}(\hat{v})x^{\hat{v}}(\hat{v})x^{2(\hat{v}-1)}(\hat{v})^{\hat{v}}(\hat{v})x^{2(\hat{v}-1)}(\hat{v})\cdots$$

$$(0)\ (2)x^3(4)\cdots(\hat{v})x^{2(\hat{v}-1)}(\hat{v})x^{\hat{v}}(\hat{v})x^{2(\hat{v}-1)}(\hat{v})^{\hat{v}}(\hat{v})x^{2(\hat{v}-1)}(\hat{v})\cdots$$

$$\vdots \qquad\qquad \vdots$$

$$(2)\ x^2(3)x^5\cdots(\hat{v})x^{\hat{v}}(\hat{v})x^{2(\hat{v}-1)}(\hat{v})x^{2\hat{v}-3}(\hat{v})x^{\hat{v}}(\hat{v})x^{\hat{v}}(\hat{v})x^{\hat{v}}(\hat{v})\cdots\cdots\cdots$$

$$(1)\ x^1(3)x^3\cdots\cdots(\hat{v})x^{\hat{v}}(\hat{v})x^{2(\hat{v}-1)}(\hat{v})x^{2\hat{v}-3}(\hat{v})x^{\hat{v}}(\hat{v})x^{\hat{v}}(\hat{v})x^{\hat{v}}(\hat{v})\cdots\cdots$$

$$(0)\ (2)x^3(4)\cdots\cdots\cdots(\hat{v})x^{\hat{v}}(\hat{v})x^{2(\hat{v}-1)}\underbrace{(\hat{v})x^{2\hat{v}-3}(\hat{v})x^{\hat{v}}(\hat{v})x^{\hat{v}}}_{\text{effect of disturbance}}(\hat{v})x^{\hat{v}}(\hat{v})\cdots$$

(b)

$$\vdots \qquad\qquad \vdots$$

$$(1)\ x^1(3)x^3\cdots(\hat{v})x^{2(\hat{v}-1)}(\hat{v})x^{\hat{v}}(\hat{v})x^{2(\hat{v}-1)}(\hat{v})^{\hat{v}}(\hat{v})x^{2(\hat{v}-1)}(\hat{v})\cdots$$

$$(0)\ (2)x^3(4)\cdots(\hat{v})x^{2(\hat{v}-1)}(\hat{v})x^{\hat{v}}(\hat{v})x^{2(\hat{v}-1)}(\hat{v})^{\hat{v}}(\hat{v})x^{2(\hat{v}-1)}(\hat{v})\cdots$$

$$(2)\ x^2(3)x^5\cdots(\hat{v})x^{2(\hat{v}-1)}(\hat{v})x^{\hat{v}}(\hat{v})x^{2(\hat{v}-1)}(\hat{v})^{\hat{v}}(\hat{v})x^{2(\hat{v}-1)}(\hat{v})\cdots$$

$(-)\ \ x^1(3)x^3\cdots(\hat{v})x^{2(\hat{v}-1)}(\hat{v})x^{\hat{v}}(\hat{v})x^{2(\hat{v}-1)}(\hat{v})^{\hat{v}}(\hat{v})x^{2(\hat{v}-1)}(\hat{v})\cdots \leftarrow$ no car

$(4)\ \ x^4(4)x^4\cdots(\hat{v})x^{2(\hat{v}-1)}(\hat{v})x^{\hat{v}}(\hat{v})x^{2(\hat{v}-1)}(\hat{v})^{\hat{v}}(\hat{v})x^{2(\hat{v}-1)}(\hat{v})\cdots$ injected!

$(3)\ \ x^3(4)x^4\cdots(\hat{v})x^{2(\hat{v}-1)}(\hat{v})x^{\hat{v}}(\hat{v})x^{2(\hat{v}-1)}(\hat{v})^{\hat{v}}(\hat{v})x^{2(\hat{v}-1)}(\hat{v})\cdots$

$(2)\ \ x^2(4)x^4\cdots(\hat{v})x^{2(\hat{v}-1)}(\hat{v})x^{\hat{v}}(\hat{v})x^{2(\hat{v}-1)}(\hat{v})^{\hat{v}}(\hat{v})x^{2(\hat{v}-1)}(\hat{v})\cdots$

$(1)\ \ x^1(3)x^4\cdots(\hat{v})x^{2(\hat{v}-1)}(\hat{v})x^{\hat{v}}(\hat{v})x^{2(\hat{v}-1)}(\hat{v})^{\hat{v}}(\hat{v})x^{2(\hat{v}-1)}(\hat{v})\cdots$

$(0)\ \ (2)x^3(4)\cdots(\hat{v})x^{2(\hat{v}-1)}(\hat{v})x^{\hat{v}}(\hat{v})x^{2(\hat{v}-1)}(\hat{v})^{\hat{v}}(\hat{v})x^{2(\hat{v}-1)}(\hat{v})\cdots$

$(2)\ \ x^2(3)x^5\cdots(\hat{v})x^{2(\hat{v}-1)}(\hat{v})x^{\hat{v}}(\hat{v})x^{2(\hat{v}-1)}(\hat{v})^{\hat{v}}(\hat{v})x^{2(\hat{v}-1)}(\hat{v})\cdots$

$(1)\ \ x^1(3)x^3\cdots(\hat{v})x^{2(\hat{v}-1)}(\hat{v})x^{\hat{v}}(\hat{v})x^{2(\hat{v}-1)}(\hat{v})^{\hat{v}}(\hat{v})x^{2(\hat{v}-1)}(\hat{v})\cdots$

$(0)\ \ (2)x^3(4)\cdots(\hat{v})x^{2(\hat{v}-1)}(\hat{v})x^{\hat{v}}(\hat{v})x^{2(\hat{v}-1)}(\hat{v})^{\hat{v}}(\hat{v})x^{2(\hat{v}-1)}(\hat{v})\cdots$

$\vdots \qquad\qquad \vdots$

$(2)\ \ x^2(3)x^5\cdots(\hat{v})x^{\hat{v}}(\hat{v})x^{2(\hat{v}-1)}(\hat{v})x^{2\hat{v}-3}(\hat{v})x^{\hat{v}}(\hat{v})x^{\hat{v}}(\hat{v})x^{\hat{v}}(\hat{v})\cdots\cdots\cdots$

$(1)\ \ x^1(3)x^3\cdots\cdots(\hat{v})x^{\hat{v}}(\hat{v})x^{2(\hat{v}-1)}(\hat{v})x^{2\hat{v}-3}(\hat{v})x^{\hat{v}}(\hat{v})x^{\hat{v}}(\hat{v})x^{\hat{v}}(\hat{v})\cdots\cdots$

$(0)\ \ (2)x^3(4)\cdots\cdots\cdots(\hat{v})x^{\hat{v}}(\hat{v})x^{2(\hat{v}-1)}\underbrace{(\hat{v})x^{2\hat{v}-3}(\hat{v})x^{\hat{v}}(\hat{v})x^{\hat{v}}}_{\text{effect of disturbance}}(\hat{v})x^{\hat{v}}(\hat{v})\cdots$

(c) $\vdots \qquad\qquad \vdots$

$(0)\ \ (2)x^3(4)\cdots(\hat{v})x^{2(\hat{v}-1)}(\hat{v})x^{\hat{v}}(\hat{v})x^{2(\hat{v}-1)}(\hat{v})^{\hat{v}}(\hat{v})x^{2(\hat{v}-1)}(\hat{v})\cdots$

$(2)\ \ x^2(3)x^5\cdots(\hat{v})x^{2(\hat{v}-1)}(\hat{v})x^{\hat{v}}(\hat{v})x^{2(\hat{v}-1)}(\hat{v})^{\hat{v}}(\hat{v})x^{2(\hat{v}-1)}(\hat{v})\cdots$

$(1)\ \ x^1(3)x^3\cdots(\hat{v})x^{2(\hat{v}-1)}(\hat{v})x^{\hat{v}}(\hat{v})x^{2(\hat{v}-1)}(\hat{v})^{\hat{v}}(\hat{v})x^{2(\hat{v}-1)}(\hat{v})\cdots$

$(-)\ \ (2)x^3(4)\cdots(\hat{v})x^{2(\hat{v}-1)}(\hat{v})x^{\hat{v}}(\hat{v})x^{2(\hat{v}-1)}(\hat{v})^{\hat{v}}(\hat{v})x^{2(\hat{v}-1)}(\hat{v})\cdots \leftarrow$ no car

$(2)\ \ x^2(3)x^5\cdots(\hat{v})x^{2(\hat{v}-1)}(\hat{v})x^{\hat{v}}(\hat{v})x^{2(\hat{v}-1)}(\hat{v})^{\hat{v}}(\hat{v})x^{2(\hat{v}-1)}(\hat{v})\cdots$ injected!

$(1)\ \ x^1(3)x^3\cdots(\hat{v})x^{2(\hat{v}-1)}(\hat{v})x^{\hat{v}}(\hat{v})x^{2(\hat{v}-1)}(\hat{v})^{\hat{v}}(\hat{v})x^{2(\hat{v}-1)}(\hat{v})\cdots$

$(0)\ \ (2)x^3(4)\cdots(\hat{v})x^{2(\hat{v}-1)}(\hat{v})x^{\hat{v}}(\hat{v})x^{2(\hat{v}-1)}(\hat{v})^{\hat{v}}(\hat{v})x^{2(\hat{v}-1)}(\hat{v})\cdots$

$\Rightarrow$no effect of disturbance

## APPENDIX B: DISTURBANCE AT THE END OF THE SYSTEM

(a) ⋮ ⋮

$\cdots x^{2(\hat{v}-1)}\ (\hat{v})\ x^{\hat{v}}\ (\hat{v})\ x^{2(\hat{v}-1)}\ (\hat{v})$

$\cdots\ (\hat{v})\ x^{2(\hat{v}-1)}\ (\hat{v})\ x^{\hat{v}}\ (\hat{v})\ x^{\hat{v}-1}$

$\cdots\ (\hat{v})\ x^{2(\hat{v}-1)}\ (\hat{v})\ x^{\hat{v}}$

$\cdots x^{2(\hat{v}-1)}\ (\hat{v})\ x^{2(\hat{v}-1)}\ (0)$ ←blockage!

$\cdots x^{2(\hat{v}-1)}\ (\hat{v})\ x^{\hat{v}}\ (\hat{v}-2)\ x^{\hat{v}-2}\ (1)$

$\cdots\ (\hat{v})\ x^{2(\hat{v}-1)}\ (\hat{v}-2)\ x^{\hat{v}-2}\ (\hat{v}-1)\ x^{1}$

$\cdots\ (\hat{v})\ x^{\hat{v}}\ (\hat{v})\ x^{2(\hat{v}-2)}\ (\hat{v}-1)\ x^{2}$----------

$\cdots\ (\hat{v})\ x^{2(\hat{v}-1)}\ (\hat{v})\ x^{\hat{v}}\ (\hat{v})\ x^{\hat{v}-1}$ from here on

$\cdots\ (\hat{v})\ x^{\hat{v}}\ (\hat{v})\ x^{2(\hat{v}-1)}\ (\hat{v})\ x^{\hat{V}}$ nothing reminds us

$\cdots x^{2(\hat{v}-1)}\ (\hat{v})\ x^{\hat{v}}\ (\hat{v})\ x^{2(\hat{v}-1)}\ (\hat{v})$ of the disturbance

(b) ⋮ ⋮

$\cdots\ (\hat{v})\ x^{2(\hat{v}-1)}\ (\hat{v})\ x^{\hat{v}}\ (\hat{v})\ x^{\hat{v}-1}$

$\cdots\ (\hat{v})\ x^{\hat{V}}\ (\hat{v})\ x^{2(\hat{v}-1)}\ (\hat{v})\ x^{\hat{v}}$

$\cdots x^{2(\hat{v}-1)}\ (\hat{v})\ x^{\hat{v}}\ (\hat{v})\ x^{2(\hat{v}-1)}\ (\hat{v})$

$\cdots\ (\hat{v})\ x^{2(\hat{v}-1)}\ (\hat{v})\ x^{\hat{v}}\ (\hat{v}-1)\ x^{\hat{v}-1}$ ←blockage!

$\cdots\ x^{\hat{v}}\ x^{2(\hat{v}-1)}(\hat{v}-1)\ x^{\hat{v}-1}\ (\hat{v})$

$\cdots\ (\hat{v})\ x^{\hat{v}}\ (\hat{v})\ x^{2\hat{v}-3}\ (\hat{v})\ x^{1}$ ----------

$\cdots\ (\hat{v})\ x^{2(\hat{v}-1)}\ (\hat{v})\ x^{\hat{v}}\ (\hat{v})\ x^{\hat{v}-1}$ from here on

$\cdots(\hat{v})\ x^{\hat{v}}\ (\hat{v})\ x^{2(\hat{v}-1)}\ (\hat{v})\ x^{\hat{v}}$ nothing reminds us

$\cdots x^{2(\hat{v}-1)}\ (\hat{v})\ x^{\hat{v}}\ (\hat{v})\ x^{2(\hat{v}-1)}\ (\hat{v})$ of the disturbance

(c) ⋮ ⋮

$\cdots\ (\hat{v})\ x^{\hat{v}}\ (\hat{v})\ x^{2(\hat{v}-1)}\ (\hat{v})\ x^{\hat{v}}$

$\cdots x^{2(\hat{v}-1)}\ (\hat{v})\ x^{\hat{v}}\ (\hat{v})\ x^{2(\hat{v}-1)}\ (\hat{v})$

$\cdots\ (\hat{v})\ x^{2(\hat{v}-1)}\ (\hat{v})\ x^{\hat{v}}\ (\hat{v})\ x^{\hat{v}-1}$

$\cdots\ (\hat{v})\ x^{\hat{v}}\ (\hat{v})\ x^{2(\hat{v}-1)}\ (\hat{v})\ x^{\hat{v}}$ ←blockage!

$\cdots x^{2(\hat{v}-1)}\ (\hat{v})\ x^{\hat{v}}\ (\hat{v})\ x^{2(\hat{v}-1)}\ (\hat{v})$ blockage

$\cdots\ (\hat{v})\ x^{2(\hat{v}-1)}\ (\hat{v})\ x^{\hat{v}}\ (\hat{v})\ x^{\hat{v}-1}$ has no

$\cdots\ (\hat{v})\ x^{\hat{v}}\ (\hat{v})\ x^{2(\hat{v}-1)}\ (\hat{v})\ x^{\hat{v}}$ effect

[1] R. K. P. Zia, B. Shaw, B. Schmittmann, and R. J. Astalos, Phys. Rep. **301**, 45 (1998).
[2] B. Schmittmann and R. P. K. Zia, e-print cond-mat/980392.
[3] J. Krug, Phys. Rev. Lett. **67**, 1882 (1991).
[4] J. Krug and P. A. Ferrari, J. Phys. A **29**, L465 (1996).
[5] B. Derrida, E. Domany, and D. Mukamel, J. Stat. Phys. **69**, 667 (1992).
[6] B. Derrida and M. R. Evans, J. Phys. I **3**, 311 (1993).
[7] B. Derrida, M. R. Evans, V. Hakim, and V. Pasquier, J. Phys. A **26**, 1493 (1993).
[8] G. Schütz and E. Domany, J. Stat. Phys. **72**, 277 (1993).
[9] N. Rajewsky and M. Schreckenberg, Physica A **245**, 139 (1997).
[10] N. Rajewsky, A. Schadschneider, and M. Schreckenberg, J. Phys. A **29**, L305 (1996).
[11] G. Schütz, Phys. Rev. E **47**, 4265 (1993).
[12] H. Hinrichsen, J. Phys. A **29**, 3659 (1996).
[13] A. Honecker and I. Peschel, J. Stat. Phys. **88**, 319 (1997).
[14] L. G. Tilstra and M. H. Ernst, J. Phys. A **31**, 5033 (1998).
[15] M. R. Evans, N. Rajewsky, and E. R. Speer, J. Stat. Phys. **95**, 45 (1999).
[16] H. Fukś and N. Boccara, Int. J. Mod. Phys. C **9**, 1 (1998).
[17] H. Fukś, Phys. Rev. E **60**, 197 (1999).
[18] J. de Gier and B. Niehnuis, Phys. Rev. E **59**, 4899 (1999).
[19] A. Benyoussef, H. Chakib, and H. Ez-Zahraouy, Eur. Phys. J. B **8**, 275 (1999).
[20] *Traffic and Granular Flow*, edited by D. E. Wolf, M. Schreckenberg, and A. Bachem (World Scientific, Singapore, 1996).
[21] *Traffic and Granular Flow '97*, edited by M. Schreckenberg and D. E. Wolf (Springer, Heidelberg, 1998).
[22] D. Chowdhury, L. Santen, and A. Schadschneider Phys. Rep. **329**, 199 (2000).
[23] N. Rajewsky, L. Santen, A. Schadschneider, and M. Schreckenberg, J. Stat. Phys. **92**, 151 (1998).
[24] K. Nagel and M. Schreckenberg, J. Phys. I **2**, 2221 (1992).
[25] M. Schreckenberg, A. Schadschneider, K. Nagel, and N. Ito, Phys. Rev. E **51**, 2939 (1995).
[26] M. Sasvári and J. Kertész, Phys. Rev. E **56**, 4104 (1997).
[27] B. Eisenblätter, L. Santen, A. Schadschneider, and M. Schreckenberg, Phys. Rev. E **57**, 1309 (1998).
[28] S. Cheybani, J. Kertész, and M. Schreckenberg, J. Phys. A **31**, 9787 (1998).
[29] L. Santen and A. Schadschneider, e-print cond-mat/9711261.
[30] L. Roters, S. Lübeck, and K. D. Usadel, Phys. Rev. E **59**, 2672 (1999).
[31] A. Schadschneider and M. Schreckenberg, J. Phys. A **26**, L679 (1993).
[32] A. Schadschneider and M. Schreckenberg, J. Phys. A **30**, L69 (1997).
[33] A. Schadschneider and M. Schreckenberg, J. Phys. A **31**, L225 (1998).
[34] A. Schadschneider, Eur. Phys. J. B **10**, 573 (1999).